Computers and Mathematics with Applications 140 (2023) 107–125

Contents lists available at ScienceDirect

Computers and Mathematics with Applications

journal homepage: www.elsevier.com/locate/camwa

Compact schemes in time with applications to partial differential equations

Stéphane Clain [a,*], Gaspar J. Machado [b,d], M.T. Malheiro [c,d]

[a] CMUC – Centre of Mathematics, Largo D. Dinis, University of Coimbra, 3000-143 Coimbra, Portugal
[b] CFUM – Centre of Physics, Azurém Campus, University of Minho, 4800-058 Guimarães, Portugal
[c] CMAT – Centre of Mathematics, Azurém Campus, University of Minho, 4800-058 Guimarães, Portugal
[d] DMAT – Department of Mathematics, Azurém Campus, University of Minho, 4800-058 Guimarães, Portugal

ARTICLE INFO

Keywords:
Compact scheme
Structural equation
Time discretization
Very high-order
A-stability
Dispersion

ABSTRACT

We propose a new class of fourth- and sixth-order schemes in time for parabolic and hyperbolic equations. The method follows the compact scheme methodology by elaborating implicit relations between the approximations of the function and its derivatives. We produce a series of A-stable methods with low dispersion and high accuracy. Several benchmarks for linear and non-linear Ordinary Differential Equations demonstrate the effectiveness of the method. Then a second set of numerical benchmarks for Partial Differential Equations such as convection-diffusion, Schrödinger equation, wave equation, Bürgers, and Euler system give the numerical evidences of the superior advantage of the method with respect to the traditional Runge-Kutta or multistep methods.

1. Introduction

Very high-order numerical methods for non-stationary Partial Differential Equations (PDEs) mainly focus on the space discretization to provide accurate and eligible discrete solutions, being the time variable usually discretized through a Runge-Kutta (RK) method or a linear multistep formulation. The focus of this work, however, is precisely the discretization in time where its assessment is not just a question of accuracy (method order), but also its stability, dissipation, dispersion (spectral resolution and phase deviation, fundamental for propagation of waves [1]), and all the computational aspects (running time, memory cost, scalability, and nowadays, the energy cost to carry out the simulation).

There is a large literature for such standard methods which we sum up in the following short notes. Gauss RK methods are all A-stable with good accuracy but suffer from a large dispersion and huge computational cost [2]. There are very few low cost A-stable Singly Diagonally RK methods, reaching at most the fourth-order of accuracy, and they present a poor spectral resolution due to a large dispersion [3]. On the other hand, implicit multistep methods (Backward Differentiation, Adams-Moulton) are A-stable up to the second order but do not produce stable solutions for oscillatory problems (linear Ordinary Differential Equations (ODEs) with imaginary coefficients) [4], or simply have a bounded stability region [3] (A-stability is not fulfilled). Implicit-Explicit RK method is another way to reduce the computational cost for problems involving two very different regimes but the dispersion is still an issue to overcome [5].

High-order discretizations in time involving several orders of derivatives have been proposed since the sixties to provide better accuracy and absolute stability. The key idea is very similar to the compact scheme principle, and consists in reducing the stencil of the neighbour nodes by adding information on the nodes such as the first-, second-, or higher derivatives. However, very few connections have been highlighted between compact schemes used in the PDE community and the implicit block multistep multi-derivative methods used in the ODE community.

The first numerical scheme in time involving second-order derivatives dates back to the ENIAC era with the so-called Clippinger and Dimsdale method (also mentioned as Iterative Simpson method) first presented in an unpublished lecture notes in 1949, unveiled in a 1952's technical note [6] and in the 1958 handbook of Grabbe, Ramo, and Woolridge [7] (chapter 14, p. 14-60). In the early 60s', Lambert and Mitchell introduced and developed in 1962 the multistep multi-derivative method [8–10] while Shampine and Watts and, independently, Axelsson introduced the block implicit one-step methods with first-order derivatives in 1969 [11–13]. At last, the implicit block multistage multi-derivative method has been suggested by Hairer and Warner in 1973 where the higher-order derivatives for future time steps are

* Corresponding author.
E-mail addresses: clain@math.uminho.pt (S. Clain), gjm@math.uminho.pt (G.J. Machado), mtm@math.uminho.pt (M.T. Malheiro).

https://doi.org/10.1016/j.camwa.2023.03.011
Received 8 July 2022; Received in revised form 9 February 2023; Accepted 17 March 2023
Available online 31 March 2023

considered in the generic formulation [14]. Actually, implicit one-step method can be formally interpreted as an implicit Runge-Kutta scheme but, paraphrasing Watts and Shampine [13], intermediate values in the RK method are rough approximations of the solution at the intermediate stages while the implicit block method delivers high accurate approximations even at the intermediate time steps. We particularly mention the two-point and three-point implicit block methods [15,16] that turn to be close to the schemes we shall propose in the present study.

Implicit block multi-derivative has been extended to second-order or higher-order differential equations [17,18] and provides a very efficient scheme while preserving the stability. Curiously, and up to the authors' knowledge, there were no applications of the implicit block method in the context of the PDEs, for instance an ODE system deriving from a simple finite difference in space of parabolic or hyperbolic operators such as the heat equation, transport, or Bürgers equation.

Since their beginning in the seventies [19], compact schemes have received important contributions to develop very high-order methods by combining function values and its derivatives over local stencils. For instance, a very good state of the art of the method is given by [20] in the late eighties. The high spectral resolution property for hermitian compact schemes has been studied by [21] and, at last, the extension to higher-order combined schemes was proposed by [22]. It is noticeable that the two approaches encompass in a common framework. Writing the two-point implicit block second-derivative method for the Initial Value Problem [23] is very similar to the three-point implicit compact combined scheme for the steady-state non-linear convection reaction Boundary Value Problem [22]. Up to the authors' knowledge, the compact scheme methodology was only developed for the space discretization, for steady state problems [24], parabolic problems [25,26], or fractional time derivatives [27,28].

We propose in the present study to revisit and adapt some compact schemes in time in the context of the non-stationary partial differential equation in the one-dimensional space. Most of the proposed schemes have a corresponding version as multi-points implicit block multi-derivative methods in the ODE context, being their application to PDEs advantageous since they provide very accurate A-stable methods. Moreover, they enjoy nice properties such as low dispersion in comparison with the popular schemes.

There are several recent methods that take advantage of the first- or second-derivative. Consider the EDO $\phi' = f(\phi,t)$, the Two-Derivative Runge-Kutta method (TDRK) [29–31] is an extension of the traditional RK method by adding new degrees of freedom with the second-derivative. Our method is very different since, on the contrary to the TDRK, we do not systematically substitute the time derivative ϕ' with $f(\phi,t)$ and the second derivative ϕ'' with $\partial_z f(\phi,t)\phi' + \partial_t f(\phi,t)$. Indeed, we consider the first- and second-derivatives ϕ', ϕ'' as unknowns together with ϕ. Moreover, we provide the same order of accuracy for ϕ, ϕ', and ϕ''.

The remaining sections of the article are organised as follows. Section 2 is dedicated to the construction and analysis of the new numerical schemes. In particular, we check the A-stability of the methods and assess the dispersion property. The numerical methods are tested in the context of ODEs in Section 3 to evaluate the accuracy, the stability, and the effective dispersion. Then we proceed in Section 4 with parabolic and hyperbolic problems. Applying a finite difference discretization in space of order eight, we are dealing with a differential system in time, where the new methods are applied. We assess the convergence, order in time, stability, and dispersion property for linear and non-linear problems. The article ends with the conclusions in Section 5.

2. Design and analysis of the compact schemes

We first consider the generic scalar first-order ODE problem

$$\phi'(t) = f(\phi(t),t),\ t \in (0,T], \tag{1}$$

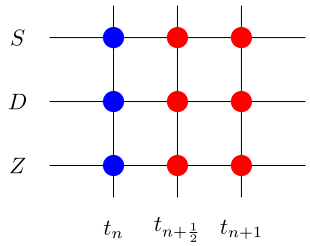

Fig. 1. Stencil: known data (•), data to compute (•).

together with the initial condition $\phi(0) = \phi_0$, with $T > 0$ the final time and $f \equiv f(z,t)$ a regular function in $\mathbb{R}\times(0,T]$. The key idea is to decompose a scheme into two subsystems of equations. The Physical Equations (PE) rely on the function and its derivatives at a node by applying the physical relations. Notice that there is no connection of information with the other nodes, since the physics is constituted of local operators. On the other hand, the Structural Equations (SE) rely on linear relations between the function and its derivatives over a stencil and fully connect a node with the neighbours. These relations are "physics" independent, since they are established independently of the problem. We address the two issues in the following sections.

2.1. Physical and structural equations

Let $N \in \mathbb{N}$, $t_n = n\Delta t$ with $n = 0,\dots,N$ and $T = N\Delta t$, and $t_{n+\frac{1}{2}} = (n+\frac{1}{2})\Delta t$ with $n = 0,\dots,N-1$. We seek approximations Z_n, D_n, and S_n for $\phi(t_n)$, $\phi'(t_n)$, and $\phi''(t_n)$, respectively, solution of equation (1). To mimic relation (1), we impose that the approximations satisfy the so-called Physical Equation (PE1) given by

$$D_n = f(Z_n,t_n), \quad n = 1,\dots,N. \tag{2}$$

Moreover, computing the derivative of equation (1) with respect to time, we obtain

$$\phi''(t) = \partial_z f(\phi(t),t)\phi'(t) + \partial_t f(\phi(t),t),$$

which provides the second Physical Equation (PE2) given by

$$S_n = \partial_z f(Z_n,t_n)D_n + \partial_t f(Z_n,t_n), \quad n = 1,\dots,N. \tag{3}$$

We now aim at establishing relations between the discrete values Z_n, D_n, and S_n and the discrete values at the next time step Z_{n+1}, D_{n+1}, and S_{n+1}. Such relations are called Structural Equations since they only depend on the structure of the grid and not on the nature of the problem. To this end, we introduce the functional

$$\begin{aligned}\mathcal{E}_n(\boldsymbol{a};\phi) = {} & a_0\phi(t_n) + a_{\frac{1}{2}}\phi(t_{n+\frac{1}{2}}) + a_1\phi(t_{n+1}) + \\ & b_0\phi'(t_n) + b_{\frac{1}{2}}\phi'(t_{n+\frac{1}{2}}) + b_1\phi'(t_{n+1}) + \\ & c_0\phi''(t_n) + c_{\frac{1}{2}}\phi''(t_{n+\frac{1}{2}}) + c_1\phi''(t_{n+1}),\end{aligned} \tag{4}$$

where

$$\boldsymbol{a} = \left(a_0, a_{\frac{1}{2}}, a_1, b_0, b_{\frac{1}{2}}, b_1, c_0, c_{\frac{1}{2}}, c_1\right) \in \mathbb{R}^9,$$

and derive the Structural Equations by determining the coefficients imposing the functional to be zero for some polynomial functions. We represent the generic stencil of the involved data in a Structural Equation in Fig. 1. The scheme is compact in the sense that we establish implicit relations between the function approximations and its derivatives (approximations of the function, first- and second-derivatives) at $t_{n+\frac{1}{2}}$ and t_{n+1}.

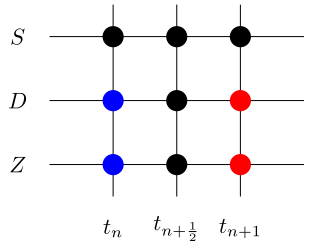

Fig. 2. Stencil: known data (•), data to compute (•), discarded data (•).

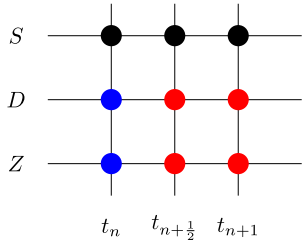

Fig. 3. Stencil: known data (•), data to compute (•), discarded data (•).

2.2. The compact scheme `[1ZD]`

To design the `[1ZD]` scheme, we impose $a_{\frac{1}{2}} = b_{\frac{1}{2}} = 0$ and $c_0 = c_{\frac{1}{2}} = c_1 = 0$. Hence the functional is reduced to (*cf.* Fig. 2)

$$\mathcal{E}_n(\boldsymbol{a};\phi) = a_0\phi(t_n) + a_1\phi(t_{n+1}) + b_0\phi'(t_n) + b_1\phi'(t_{n+1}).$$

We seek coefficients a_0, a_1, b_0, b_1 such that $\mathcal{E}_n(\boldsymbol{a};\phi) = 0$ for polynomials $\phi(t) = t^\alpha$, $\alpha = 0, 1, 2$, deducing a solution (up to a multiplicative constant) which is given by

$$a_0 = \frac{1}{\Delta t},\ a_1 = -\frac{1}{\Delta t},\ b_0 = \frac{1}{2},\ b_1 = \frac{1}{2},$$

that provides the Structural Equation

$$\frac{D_{n+1} + D_n}{2} - \frac{Z_{n+1} - Z_n}{\Delta t} = 0. \tag{5}$$

The `[1ZD]` scheme is given by combining the Physical Equation (2) at time t_{n+1} and the Structural Equation (5), and reads: given (Z_n, D_n), compute (Z_{n+1}, D_{n+1}) such that

$$\begin{aligned} &D_{n+1} - f(Z_{n+1}, t_{n+1}) = 0,\\ &\frac{D_{n+1} + D_n}{2} - \frac{Z_{n+1} - Z_n}{\Delta t} = 0. \end{aligned}$$

We here obtain the popular A-stable Crank-Nicholson method, that we tag by `[CN]`. Indeed, considering the linear equation $\phi' = \lambda\phi$ with $\lambda \in \mathbb{C}$, then one has

$$Z_{n+1} = A(ß)Z_n, \qquad A(ß) = \frac{2 + ß}{2 - ß},$$

with A the transfer function and $ß = \lambda\Delta t$. We check that $|A(ß)| \le 1$ if $\mathrm{Re}(\lambda) \le 0$ and deduce that the scheme enjoys the A-stability property.

2.3. The compact scheme `[2ZD]`

We introduce an intermediate point at $t_{n+\frac{1}{2}}$ together with the associated approximations $Z_{n+\frac{1}{2}}$ and $D_{n+\frac{1}{2}}$ but cancelling the second-derivative terms, that is, considering $c_0 = c_{\frac{1}{2}} = c_1 = 0$. The functional then reads (*cf.* Fig. 3)

$$\begin{aligned} \mathcal{E}_n(\boldsymbol{a};\phi) = {} & a_0\phi(t_n) + a_{\frac{1}{2}}\phi(t_{n+\frac{1}{2}}) + a_1\phi(t_{n+1}) + b_0\phi'(t_n) + b_{\frac{1}{2}}\phi'(t_{n+\frac{1}{2}})\\ & + b_1\phi'(t_{n+1}). \end{aligned}$$

Prescribing $\mathcal{E}_n(\boldsymbol{a};\phi) = 0$ for polynomials $\phi(t) = t^\alpha$, $\alpha = 0, \dots, 4$, leads to the fourth-order Structural Equation

$$-6\frac{Z_{n+1} - Z_n}{\Delta t} + (D_n + 4D_{n+\frac{1}{2}} + D_{n+1}) = 0. \tag{6}$$

Moreover, if one relaxes the constraints by cancelling the relation $\mathcal{E}_n(\boldsymbol{a};t^4) = 0$, we obtain a second Structural Equation (SE2) that reads

$$-4\frac{Z_n - 2Z_{n+\frac{1}{2}} + Z_{n+1}}{\Delta t} + (D_{n+1} - D_n) = 0. \tag{7}$$

We then combine the Physical Equation (2) at time $t_{n+\frac{1}{2}}$ and t_{n+1} together with the two Structural Equations (6)-(7). Assuming that Z_n, D_n are known, we aim at computing $Z_{n+\frac{1}{2}}$, $D_{n+\frac{1}{2}}$, Z_{n+1}, D_{n+1} using the `[2ZD]` scheme

$$\begin{aligned} &-\frac{Z_{n+1} - Z_n}{\Delta t} + \frac{D_n + 4D_{n+\frac{1}{2}} + D_{n+1}}{6} = 0,\\ &-\frac{Z_n - 2Z_{n+\frac{1}{2}} + Z_{n+1}}{\Delta t} + \frac{D_{n+1} - D_n}{4} = 0,\\ &D_{n+\frac{1}{2}} - f(Z_{n+\frac{1}{2}}, t_{n+\frac{1}{2}}) = 0,\\ &D_{n+1} - f(Z_{n+1}, t_{n+1}) = 0. \end{aligned}$$

The scheme is equivalent to the one-step implicit block method of Shampine and Watts [12,13], Axelsson [11] for first-order ODE.

Linear stability of scheme `[2ZD]` To study the linear stability of the scheme, we consider the linear differential equation $\phi' = \lambda\phi$, *i.e.* $f(z,t) = \lambda z$, $\lambda \in \mathbb{C}$. By substituting the derivative in the Structural Equations, we get

$$\begin{aligned} &-6(Z_{n+1} - Z_n) + \lambda\Delta t(Z_n + 4Z_{n+\frac{1}{2}} + Z_{n+1}) = 0,\\ &-4(Z_n - 2Z_{n+\frac{1}{2}} + Z_{n+1}) + \lambda\Delta t(Z_{n+1} - Z_n) = 0. \end{aligned}$$

Setting $ß = \lambda\Delta t$, we rewrite the problem as the linear system

$$\begin{bmatrix} 6 - ß & -4ß \\ 4 - ß & -8 \end{bmatrix} \begin{bmatrix} Z_{n+1} \\ Z_{n+\frac{1}{2}} \end{bmatrix} = \begin{bmatrix} 6 + ß \\ -ß - 4 \end{bmatrix} Z_n,$$

and, using the Cramer's method, we get

$$Z_{n+1} = A(ß)Z_n,\ Z_{n+\frac{1}{2}} = B(ß)Z_n,$$

with

$$A(ß) = \frac{12 + 6ß + ß^2}{12 - 6ß + ß^2}, \quad B(ß) = \frac{24 - ß^2}{24 - 12ß + 2ß^2}.$$

Stability is then achieved for the sub-domain

$$R = \{ß \in \mathbb{C}; |A(ß)| \le 1\}.$$

Proposition 2.1. *Assume that $\lambda \in]-\infty, 0]$. Then the scheme is unconditionally stable, and we have $|Z_n| \le |Z_0|$.*

Proof. Assume that $\lambda \in]-\infty, 0]$. We have

$$A(ß) = \frac{3 + (ß + 3)^2}{3 + (ß - 3)^2} \in]0, 1].$$

Since $\lambda \le 0$, we have $(ß + 3)^2 \le (ß - 3)^2$ hence, $|Z_{n+1}| \le |Z_n|$ and by induction $|Z_n| \le |Z_0|$. We conclude that the scheme is unconditionally stable. □

Extending the stability region to the whole left half-plane, we have the following result.

Proposition 2.2. *We have $R = \{ß \in \mathbb{C};\ \mathrm{Re}(ß) \le 0\}$, i.e. the scheme is A-stable.*

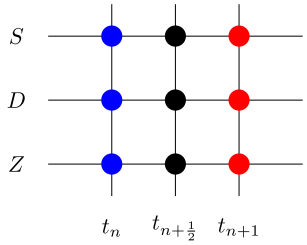

Fig. 4. Stencil: known data (•), data to compute (•), discarded data (•).

Proof. We determine the boundary of R using the equation

$$\left|A(ß)\right| = \left|\frac{3+(ß+3)^2}{3+(ß-3)^2}\right| = 1.$$

Considering the conjugate expression, we obtain the equivalent condition

$$ß(12+\bar{ß}^2)+\bar{ß}(12+ß^2)=0,$$

which indicates that the real part is null, *i.e.* $\mathrm{Re}(ß(12+\bar{ß}^2))=0$. Setting $ß = x+\mathrm{i}y$, we get the equivalent relation $x(12+x^2+y^2)=0$. Hence, the imaginary axis is the boundary of the stability region R, obtaining the conclusion. □

2.4. The compact scheme [1ZDS]

Another way to provide a fourth-order scheme consists in introducing the second derivative. To this end, we cancel the coefficients $a_{\frac{1}{2}} = b_{\frac{1}{2}} = c_{\frac{1}{2}} = 0$ and the functional (4) reads (*cf.* Fig. 4)

$$\mathcal{E}_n(\boldsymbol{a};\phi) = a_0\phi(t_n)+a_1\phi(t_{n+1})+b_0\phi'(t_n)+b_1\phi'(t_{n+1})+c_0\phi''(t_n)+c_1\phi''(t_{n+1}).$$

We impose $\mathcal{E}_n(\boldsymbol{a};\phi)=0$ for $\phi(t)=t^\alpha$, $\alpha=0,\dots,4$, and we get the Structural Equation (SE1)

$$12\frac{Z_n-Z_{n+1}}{(\Delta t)^2}+6\frac{D_n+D_{n+1}}{\Delta t}+(S_n-S_{n+1})=0. \tag{9}$$

Together with the two Physical Equations (2)-(3) at point t_{n+1}, we get the compact scheme [1ZDS]. Given approximations Z_n, D_n, S_n of ϕ and their derivatives at time t_n, we aim at determining the approximations Z_{n+1}, D_{n+1}, S_{n+1} at time t_{n+1} such that

$$12\frac{Z_n-Z_{n+1}}{(\Delta t)^2}+6\frac{D_n+D_{n+1}}{\Delta t}+(S_n-S_{n+1})=0,$$
$$D_{n+1}-f(Z_{n+1},t_{n+1})=0,$$
$$S_{n+1}-\partial_z f(Z_{n+1},t_{n+1})D_{n+1}+\partial_t f(Z_{n+1},t_{n+1})=0.$$

We recover the multistep multi-derivative method proposed by Lambert and Mitchell [8–10].

Linear stability of scheme [1ZDS] Taking $f(z)=\lambda z$ with $\lambda\in\mathbb{C}$ and denoting $ß=\lambda\Delta t$, substitution in the Structural Equation (SE1) gives

$$12(Z_n-Z_{n+1})+6ß(Z_n+Z_{n+1})+ß^2(Z_n-Z_{n+1})=0$$

which is equivalent to

$$Z_{n+1}\left(12-6ß+ß^2\right)=Z_n\left(12+6ß+ß^2\right)\ \Rightarrow Z_{n+1}=A(ß)Z_n$$

with

$$A(ß)=\frac{3+(ß+3)^2}{3+(ß-3)^2}\in\,]0,1].$$

The noticeable point is that function A is exactly the same as in the [2ZD], hence we get the same A-stability property.

2.5. The compact scheme [2ZDS]

We introduce once again the intermediate point at $t_{n+\frac{1}{2}}$ now dealing with the full functional (4) with nine coefficients.

Since we require two Structural Equations, we demand for two degrees of freedom prescribing $\mathcal{E}_n(\boldsymbol{a};\phi)=0$ for functions $\phi(t)=t^\alpha$, $\alpha=0,\dots,6$, that provide two sets of coefficients up to a multiplicative constant. The two Structural Equations then read

$$16\frac{Z_{n+1}-2Z_{n+\frac{1}{2}}+Z_n}{(\Delta t)^2}-3\frac{D_{n+1}-D_n}{\Delta t}+\frac{S_{n+1}-8S_{n+\frac{1}{2}}+S_n}{6}=0,$$
$$30\frac{Z_{n+1}-Z_n}{(\Delta t)^2}-\frac{7D_{n+1}+16D_{n+\frac{1}{2}}+7D_n}{\Delta t}+\frac{S_{n+1}-S_n}{2}=0.$$

Additionally, the Physical Equations (2)-(3) at point $t_{n+\frac{1}{2}}$ and t_{n+1} have to be fulfilled. Assuming that Z_n, D_n, S_n are known, we aim at computing $Z_{n+\frac{1}{2}}$, $D_{n+\frac{1}{2}}$, $S_{n+\frac{1}{2}}$, Z_{n+1}, D_{n+1}, S_{n+1} given by the [2ZDS] scheme

$$16\frac{Z_{n+1}-2Z_{n+\frac{1}{2}}+Z_n}{(\Delta t)^2}-3\frac{D_{n+1}-D_n}{\Delta t}+\frac{S_{n+1}-8S_{n+\frac{1}{2}}+S_n}{6}=0,$$
$$30\frac{Z_{n+1}-Z_n}{(\Delta t)^2}-\frac{7D_{n+1}+16D_{n+\frac{1}{2}}+7D_n}{\Delta t}+\frac{S_{n+1}-S_n}{2}=0,$$
$$D_{n+\frac{1}{2}}-f(Z_{n+\frac{1}{2}})=0,$$
$$S_{n+\frac{1}{2}}-\partial_z f(Z_{n+\frac{1}{2}},t_{n+\frac{1}{2}})D_{n+\frac{1}{2}}-\partial_t f(Z_{n+\frac{1}{2}},t_{n+\frac{1}{2}})=0,$$
$$D_{n+1}-f(Z_{n+1})=0,$$
$$S_{n+1}-\partial_z f(Z_{n+1},t_{n+1})D_{n+1}-\partial_t f(Z_{n+1},t_{n+1})=0.$$

We obtain a scheme that corresponds to a two-step implicit block method recently developed for the ODEs' framework [16].

Linear stability of scheme [2ZDS] Taking $f(z)=\lambda z$ with $\lambda\in\mathbb{C}$, substitution in the Structural Equations (SE1) and (SE2) gives

$$16(Z_{n+1}-2Z_{n+\frac{1}{2}}+Z_n)-3ß(Z_{n+1}-Z_n)+\frac{ß^2}{6}(Z_{n+1}-8Z_{n+\frac{1}{2}}+Z_n)=0,$$
$$30(Z_{n+1}-Z_n)-ß(7Z_{n+1}+16Z_{n+\frac{1}{2}}+7Z_n)+\frac{ß^2}{2}(Z_{n+1}-Z_n)=0,$$

which can be rewritten in the matrix form

$$\begin{bmatrix}32+\frac{4ß^2}{3} & -16+3ß-\frac{ß^2}{6}\\ -16ß & 30-7ß+\frac{ß^2}{2}\end{bmatrix}\begin{bmatrix}Z_{n+\frac{1}{2}}\\ Z_{n+1}\end{bmatrix}=\begin{bmatrix}16+3ß+\frac{ß^2}{6}\\ 30+7ß+\frac{ß^2}{2}\end{bmatrix}Z_n.$$

Expressions for $Z_{n+\frac{1}{2}}$ and Z_{n+1} are then given by

$$Z_{n+\frac{1}{2}}=\frac{\pi_1(ß)}{\pi_0(ß)}Z_n,\qquad Z_{n+1}=\frac{\pi_2(ß)}{\pi_0(ß)}Z_n,$$

with

$$\pi_0(ß)=\frac{2ß^4-36ß^3}{3}+104ß^2-480ß+960,$$
$$\pi_1(ß)=\frac{ß^2\left(ß^2-96\right)}{6}+960,$$
$$\pi_2(ß)=\frac{2ß^4+36ß^3}{3}+104ß^2+480ß+960.$$

Proposition 2.3. *Assume that $\lambda\in]-\infty,0]$. Then the scheme is unconditionally stable, and we have $|Z_n|\le|Z_0|$.*

Proof. Since $ß\le 0$, we deduce that $|\pi_2(ß)|\le|\pi_0(ß)|$, thus $|Z_{n+1}|\le|Z_n|$. The final inequality is simply obtained by induction and we conclude that the scheme is unconditionally stable. □

Proposition 2.4. *We have* $R = \{ß \in \mathbb{C};\ \mathrm{Re}(ß) \le 0\}$, *i.e. the scheme is A-stable.*

Proof. We determine the boundary of R with the equation

$$|\pi_2(ß)| = |\pi_0(ß)|.$$

And using the conjugate expression, we obtain the equivalent condition

$$\mathrm{Re}(ß)\left((ß\bar{ß})^3 + 156(ß\bar{ß})^2 + 6240(ß\bar{ß}) + 57600\right) + 2\,\mathrm{Re}(ß)^3\left(20(ß\bar{ß}) + 720\right) = 0.$$

Setting $ß = x + \mathrm{i}y$ with $x, y \in \mathbb{R}$ we get the equivalent relation

$$x\left(x^6 + y^6 + 3x^2y^4 + 3x^4y^2 + 196x^4 + 36y^4 + 232x^2y^2 + 7680x^2 + 1920y^2 + 57600\right) = 0.$$

The polynomial of degree 6 is a sum of monomials of order pair with an independent term, so this equation is equivalent to $x = 0$. Hence, the imaginary axis is the boundary of the stability region R, thus the conclusion. □

2.6. An original compact scheme [2ZDS'] and its extension [2ZDS"]

Each previous scheme has an equivalent expression in the context of ODE methods. The common feature is the systematic usage of a Physical Equation to substitute the first- or second-derivatives. We here propose an original scheme that does not have any equivalent with respect to the ODE methods. We consider two additional Structural Equations in place of the Physical Equation (PE2) at $t = t_{n+1/2}$ and $t = t_{n+1}$. These conditions are obtained by reducing the number of constraints of the functional to provide two Structural Equations. The [2ZDS'] scheme reads

$$16\frac{Z_{n+1} - 2Z_{n+\frac{1}{2}} + Z_n}{(\Delta t)^2} - 3\frac{D_{n+1} - D_n}{\Delta t} + \frac{S_{n+1} - 8S_{n+\frac{1}{2}} + S_n}{6} = 0,$$

$$30\frac{Z_{n+1} - Z_n}{(\Delta t)^2} - \frac{7D_{n+1} + 16D_{n+\frac{1}{2}} + 7D_n}{\Delta t} + \frac{S_{n+1} - S_n}{2} = 0,$$

$$-8\frac{Z_{n+1} - 2Z_{n+\frac{1}{2}} + Z_n}{(\Delta t)^2} + \frac{D_{n+1} - D_n}{\Delta t} + S_{n+\frac{1}{2}} = 0,$$

$$12\frac{Z_{n+1} - Z_n}{(\Delta t)^2} - 2\frac{D_{n+1} + 4D_{n+\frac{1}{2}} + D_n}{\Delta t} = 0,$$

$$D_{n+1} - f(Z_{n+1}) = 0,$$

$$D_{n+\frac{1}{2}} - f(Z_{n+\frac{1}{2}}) = 0.$$

Two Physical Equations are stated for the first-derivatives, but not for the second-derivatives. We then obtain a prediction for $S_{n+\frac{1}{2}}$ and S_{n+1}.

We elaborate an alternative scheme, tagged [2ZDS"], by reevaluating a new approximation for S_{n+1} using (PE2), but performed *a posteriori*. The resolution of the non-linear system does not involve the second Physical Equation, but its application *a posteriori* strongly improves the second derivative accuracy and the stability.

Linear stability of scheme [2ZDS"] To assess the stability, we take $f(z) = \lambda z$ and one has $D_{n+\alpha} = \lambda Z_{n+\alpha}$, $\alpha = 0, \frac{1}{2}, 1$ (notice that we also have $S_n = \lambda^2 Z_n$ but such relation do not hold any longer for $n + \frac{1}{2}$ and $n + 1$). Substituting in the four Structural Equations, we have

$$16(Z_{n+1} - 2Z_{n+\frac{1}{2}} + Z_n) - 3ß(Z_{n+1} - Z_n) + \frac{ß^2}{6}\left(\frac{S_{n+1}}{\lambda^2} - 8\frac{S_{n+\frac{1}{2}}}{\lambda^2} + Z_n\right) = 0,$$

$$30(Z_{n+1} - Z_n) - ß(7Z_{n+1} + 16Z_{n+\frac{1}{2}} + 7Z_n) + \frac{ß^2}{2}\left(\frac{S_{n+1}}{\lambda^2} - Z_n\right) = 0,$$

$$-8(Z_{n+1} - 2Z_{n+\frac{1}{2}} + Z_n) + ß(Z_{n+1} - Z_n) + ß^2\frac{S_{n+\frac{1}{2}}}{\lambda^2} = 0,$$

$$12(Z_{n+1} - Z_n) - 2ß(Z_{n+1} + 4Z_{n+\frac{1}{2}} + Z_n) = 0.$$

Reformulating the problem under the matrix form

$$\begin{bmatrix} -32 & 16 - 3ß & -\frac{4}{3}ß^2 & \frac{1}{6}ß^2 \\ -16ß & 30 - 7ß & 0 & \frac{1}{2}ß^2 \\ 16 & -8 + ß & ß^2 & 0 \\ -8ß & 12 - 2ß & 0 & 0 \end{bmatrix} \begin{bmatrix} Z_{n+\frac{1}{2}} \\ Z_{n+1} \\ \frac{1}{\lambda^2}S_{n+\frac{1}{2}} \\ \frac{1}{\lambda^2}S_{n+1} \end{bmatrix} = \begin{bmatrix} -16 - 3ß - \frac{1}{6}ß^2 \\ 30 + 7ß + \frac{1}{2}ß^2 \\ 8 + ß \\ 12 + 2ß \end{bmatrix} Z_n,$$

and now using Crammer's rule, we compute Z_{n+1} in function of Z_n and get $Z_{n+1} = A(ß)Z_n$ with the transfer function given by

$$A(ß) = \frac{\frac{4}{3}ß^3 + \frac{32}{3}ß^2 + 40ß + 64}{\frac{8}{3}ß^2 - 24ß + 64}.$$

The stability condition is given by the condition $|A(ß)| \le 1$ and Fig. 5 displays the level-set $|A(ß)| = 1$ together with the [RK4] one for the sake of comparison. When ß is pure imaginary number ($ß = \mathrm{i}\kappa$ for $\kappa \in \mathbb{R}$), we have that $|A(ß)| \ge 1$, where $|A(ß)| = 1$ if and only if $ß = 0$.

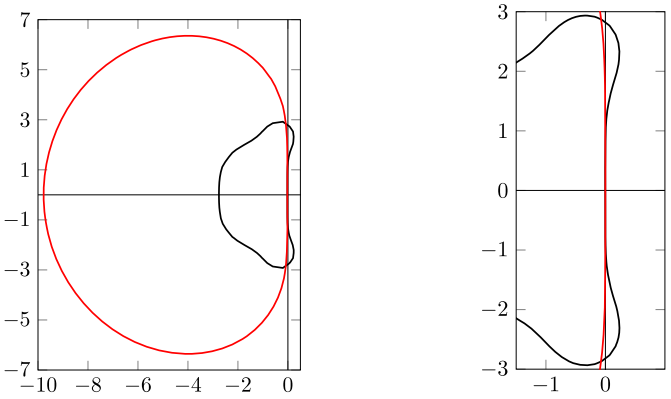

Fig. 5. Stability region for the [2ZDS"] scheme (——) and comparison with the [RK4] stability region (——).

2.7. Diffusion and dispersion analysis

To assess the diffusion and dispersion of the schemes, we consider the ODE $\phi' = \mathrm{i}\kappa\phi$, $\kappa > 0$, with solution $\phi(t) = \exp(\mathrm{i}\kappa t)$. Assume that $Z_n = \exp(\mathrm{i}\kappa n\Delta t)$ is the exact solution. Applying the numerical scheme we obtain the approximation at t_{n+1} given by $Z_{n+1} = \chi\exp(\mathrm{i}\kappa(n+1)\Delta t)$, where $\chi \in \mathbb{C}$ represents the deviation with respect to the exact solution. The ideal situation corresponds to $\chi = 1$ but in practice the deviation χ depends on $\omega = \kappa\Delta t$. We characterize the numerical error in two ways: $\arg(\chi)$ quantifies the dispersion while $|\chi|$ quantifies the diffusion.

We recall that the transfer function $A(ß)$ has been defined for the stability issue by $Z_{n+1} = A(ß)Z_n$. Taking the particular case $ß = \mathrm{i}\kappa\Delta t = \mathrm{i}\omega$, we get the relation

$$\chi(\omega) = A(\mathrm{i}\omega)\ \exp(-\mathrm{i}\omega).$$

Hence we easily deduce the χ function for the five schemes considered above:

- For [1ZD], the function χ reads
$$\chi(\omega) = \frac{2 + \mathrm{i}\omega}{2 - \mathrm{i}\omega}\ \exp(-\mathrm{i}\omega).$$
- For [2ZD] and [1ZDS], the χ function is the same and reads
$$\chi(\omega) = \frac{12 + \mathrm{i}6\omega - \omega^2}{12 - \mathrm{i}6\omega - \omega^2}\ \exp(-\mathrm{i}\omega).$$

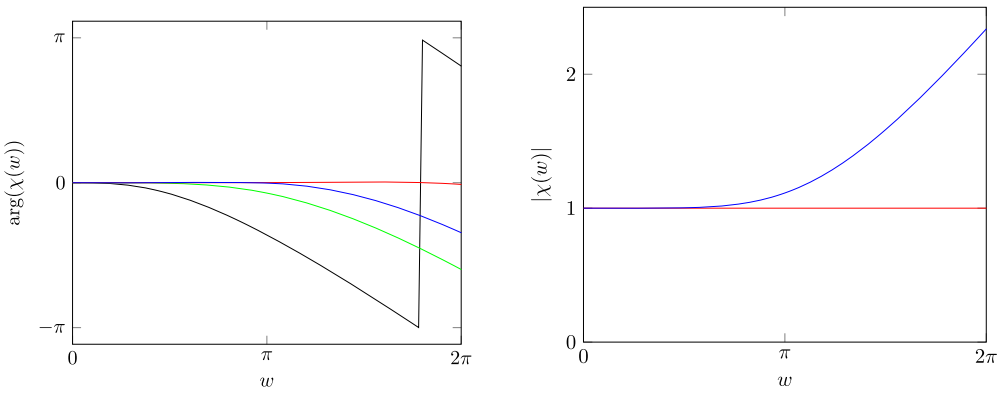

Fig. 6. Left panel: dispersion curves $\arg(\chi)$ in function of ω for schemes `[CN]` (—), `[2ZD]` (—), `[2ZDS]` (—), and `[2ZDS″]` (—). The `[2ZDS]` clearly achieves an excellent spectral resolution even for large values ω. Right Panel: dissipation curves for $|\chi|$ in function of ω for schemes `[CN]`, `[2ZD]`, `[2ZDS]` (—) and `[2ZDS″]` (—). All the centred schemes are non-dissipative except scheme `[2ZDS″]` that presents an anti-diffusion behaviour.

- For `[2ZDS]`, we obtain

$$\chi(\omega) = \frac{2\omega^4 - 36\mathrm{i}\omega^3 - 312\omega^2 + 1440\mathrm{i}\omega + 2880}{2\omega^4 + 36\mathrm{i}\omega^3 - 312\omega^2 - 1440\mathrm{i}\omega + 2880}\ \exp(-\mathrm{i}\omega).$$

- For `[2ZDS″]`, we finally get

$$\chi(\omega) = \frac{-4\mathrm{i}\omega^3 - 32\omega^2 + 120\mathrm{i}\omega + 192}{-8\omega^2 - 72\mathrm{i}\omega + 192}\ \exp(-\mathrm{i}\omega).$$

We plot in Fig. 6 the dispersion curve $\arg(\chi)$ (left panel) and the diffusion curve $|\chi|$ (right panel) in function of ω on the interval $[0, 2\pi]$. We underline the very good performance of the `[2ZDS″]` and the excellent behaviour of `[2ZDS]` to prevent from phase deviation. All the centred schemes present no dissipation ($|\chi| = 1$), except the `[2ZDS″]` method that produces an amplification of the signal corresponding to an anti-diffusive scheme.

3. Benchmarking for ordinary differential equations

To assess the errors and the convergence rate at the final time, we define

$$E(N) = |Z_N - \phi(T)|,$$

where Z_N is the numerical approximation at time $t_N = N\Delta t = T$ while the rate of convergence between two numerical solutions ϕ^{N_1} and ϕ^{N_2} reads

$$O(N_1, N_2) = \frac{\left|\log\left[E(N_1)/E(N_2)\right]\right|}{|\log N_1/N_2|}.$$

Since we will consider that solutions are regular we assess the error all along the timeline in L_∞ norm given by

$$E_\infty(N) = \max_{n=0}^{N} \left|Z_n - \phi(t_n)\right|,$$

where Z_n is the numerical approximation at time $t = t_n$. We derive the rate of convergence by

$$O_\infty(N_1, N_2) = \frac{\left|\log\left[E_\infty(N_1)/E_\infty(N_2)\right]\right|}{\left|\log N_1/N_2\right|}.$$

The equivalent expressions for D and S are also considered.

The parts of the convergence tables regarding D and S for scheme `[CN]` and S for scheme `[2ZD]` are computed *a posteriori* and printed in blue.. (For interpretation of the colours in the tables, the reader is referred to the web version of this article.)

Table 1
Benchmark ODE1.

time scheme	N	Z		D		S	
		E	O	E	O	E	O
`[2ZD]`	2	3.24E−05	—	3.24E−05	—	3.24E−05	—
	4	2.00E−06	4.02	2.00E−06	4.02	2.00E−06	4.02
	6	3.95E−07	4.01	3.95E−07	4.01	3.95E−07	4.01
	8	1.25E−07	4.00	1.25E−07	4.00	1.25E−07	4.00
`[1ZDS]`	2	3.24E−05	—	3.24E−05	—	3.24E−05	—
	4	2.00E−06	4.02	2.00E−06	4.02	2.00E−06	4.02
	6	3.95E−07	4.01	3.95E−07	4.01	3.95E−07	4.01
	8	1.25E−07	4.00	1.25E−07	4.00	1.25E−07	4.00
`[2ZDS]`	2	9.64E−09	—	9.64E−09	—	9.64E−09	—
	4	1.49E−10	6.02	1.49E−10	6.02	1.49E−10	6.02
	6	1.31E−11	6.01	1.31E−11	6.01	1.31E−11	6.01
	8	2.32E−12	6.00	2.32E−12	6.00	2.32E−12	6.00
`[2ZDS′]`	2	1.55E−05	—	1.55E−05	—	3.77E−03	—
	4	9.88E−07	3.98	9.88E−07	3.98	9.51E−04	1.99
	6	1.96E−07	3.99	1.96E−07	3.99	4.23E−04	2.00
	8	6.20E−08	4.00	6.20E−08	4.00	2.38E−04	2.00
`[2ZDS″]`	2	1.08E−05	—	1.08E−05	—	1.08E−05	—
	4	5.82E−07	4.22	5.82E−07	4.22	5.82E−07	4.22
	6	1.09E−07	4.13	1.09E−07	4.13	1.09E−07	4.13
	8	3.37E−08	4.09	3.37E−08	4.09	3.37E−08	4.09

3.1. Benchmark ODE1

We consider the linear equation $\phi' = -\phi$ in $(0, T]$ with $\phi(0) = 1$ to assess the numerical diffusion. We carry out numerical simulations up to the final time $T = 1$ with $N = 2, 4, 6, 8$ using the five schemes `[2ZD]`, `[1ZDS]`, `[2ZDS]`, `[2ZDS′]`, and `[2ZDS″]` and compare them with the exact solution $\phi(t) = \exp(-t)$. We report in Table 1 the errors at the final time together with the convergence order. The expected fourth-order for the `[2ZD]`, `[1ZDS]`, and `[2ZDS″]` is achieved while we obtain an effective sixth-order of convergence with the `[2ZDS]` scheme for Z, D, and S. With the scheme `[2ZDS′]` we obtain the expected fourth-order for Z and D and second-order for S. Notice the difference of the convergence rate between the original `[2ZDS′]` scheme and its extension `[2ZDS″]`.

3.2. Benchmark ODE2

To assess the spectral resolution of the scheme, we consider the linear equation $\phi' = -\mathrm{i}2k\pi\phi$ in $(0, T]$ with $\phi(0) = 1$ where $k \in \mathbb{N}$ is the wave number and i the imaginary unit. We evaluate the dispersion between the numerical approximation and the exact solution $\phi(t) = \exp(\mathrm{i}2k\pi t)$. We take $k = 5$ for the first case (benchmark ODE2a)

Table 2
Benchmark ODE2a.

time scheme	N	Z		D		S	
		E	O	E	O	E	O
[CN]	20	1.36E+00	—	4.28E+01	—	1.34E+03	—
	30	1.89E+00	—	5.94E+01	—	1.87E+03	—
	200	6.43E−02	1.78	2.02E+00	1.78	6.35E+01	1.78
	300	2.87E−02	1.99	9.00E−01	1.99	2.83E+01	1.99
[2ZD]	20	2.27E−01	—	7.13E+00	—	2.24E+02	—
	30	4.91E−02	3.78	1.54E+00	3.78	4.84E+01	3.78
	200	2.65E−05	3.97	8.33E−04	3.97	2.62E−02	3.97
	300	5.24E−06	4.00	1.65E−04	4.00	5.18E−03	4.00
[1ZDS]	20	2.27E−01	—	7.13E+00	—	2.24E+02	—
	30	4.91E−02	3.78	1.54E+00	3.78	4.84E+01	3.78
	200	2.65E−05	3.97	8.33E−04	3.97	2.62E−02	3.97
	300	5.24E−06	4.00	1.65E−04	4.00	5.18E−03	4.00
[2ZDS]	20	6.74E−04	—	2.12E−02	—	6.65E−01	—
	30	6.42E−05	5.80	2.02E−03	5.80	6.34E−02	5.80
	200	7.79E−10	5.97	2.45E−08	5.97	7.69E−07	5.97
	300	6.85E−11	6.00	2.15E−09	6.00	6.76E−08	6.00
[2ZDS′]	20	8.63E−03	—	2.71E−01	—	7.94E+01	—
	30	9.94E−04	5.33	3.12E−02	5.33	2.92E+01	2.47
	200	2.44E−07	4.38	7.68E−06	4.38	5.76E−01	2.07
	300	4.77E−08	4.03	1.50E−06	4.03	2.55E−01	2.00
[2ZDS″]	20	7.31E−02	—	2.30E+00	—	7.22E+01	—
	30	1.37E−02	4.13	4.30E−01	4.13	1.35E+01	4.13
	200	6.65E−06	4.02	2.09E−04	4.02	6.56E−03	4.02
	300	1.31E−06	4.00	4.12E−05	4.00	1.30E−03	4.00

Table 3
Benchmark ODE2b.

time scheme	N	Z		D		S	
		E	O	E	O	E	O
[CN]	20	1.88E+00	—	1.18E+02	—	7.44E+03	—
	30	1.54E+00	0.50	9.68E+01	0.50	6.08E+03	0.50
	200	5.04E−01	0.59	3.17E+01	0.59	1.99E+03	0.59
	300	2.28E−01	1.96	1.43E+01	1.96	8.99E+02	1.96
[2ZD]	20	1.56E+00	—	9.77E+01	—	6.14E+03	—
	30	1.18E+00	0.67	7.44E+01	0.67	4.67E+03	0.67
	200	8.45E−04	3.82	5.31E−02	3.82	3.34E+00	3.82
	300	1.67E−04	3.99	1.05E−02	3.99	6.61E−01	3.99
[1ZDS]	20	1.56E+00	—	9.77E+01	—	6.14E+03	—
	30	1.18E+00	0.67	7.44E+01	0.67	4.67E+03	0.67
	200	8.45E−04	3.82	5.31E−02	3.82	3.34E+00	3.82
	300	1.67E−04	3.99	1.05E−02	3.99	6.61E−01	3.99
[2ZDS]	20	5.28E−02	—	3.32E+00	—	2.08E+02	—
	30	6.72E−03	5.09	4.22E−01	5.09	2.65E+01	5.09
	200	9.93E−08	5.86	6.24E−06	5.86	3.92E−04	5.86
	300	8.75E−09	5.99	5.50E−07	5.99	3.45E−05	5.99
[2ZDS′]	20	1.03E+00	—	6.47E+01	—	5.63E+03	—
	30	6.57E−02	6.79	4.13E+00	6.79	4.76E+02	6.09
	200	5.50E−06	4.95	3.45E−04	4.95	1.31E+01	1.90
	300	1.07E−06	4.03	6.75E−05	4.03	5.78E+00	2.01
[2ZDS″]	20	7.65E+00	—	4.81E+02	—	3.02E+04	—
	30	5.67E−01	6.42	3.56E+01	6.42	2.24E+03	6.42
	200	2.13E−04	4.16	1.34E−02	4.16	8.42E−01	4.16
	300	4.21E−05	4.01	2.64E−03	4.01	1.66E−01	4.01

and a higher frequency $k = 10$ for the second case (benchmark ODE2b). We carry out numerical simulations up to the final time $T = 1$, with $N = 20, 30, 200, 300$. Errors and convergence orders are reported in Tables 2 and 3, for each case respectively. The Crank-Nicholson scheme has been added for the sake of comparison. As expected, the [CN] provides a second-order scheme while the compact schemes [2ZD], [1ZDS] guarantee a fourth-order of accuracy. With the scheme [2ZDS′] we obtain the expected fourth-order for Z and D and second-order for S. At last, the very efficient [2ZDS] delivers an effective sixth-order scheme that highlights the capacity to strongly reduce the dispersion. To confirm the dispersion assessment, we take $k = 10$ and plot the solution over the whole interval $[0, T]$ for $I = 20$ in Fig. 7 and $I = 40$ in Fig. 8 to assess the phase deviation between the exact solution and the approximations.

3.3. Benchmark ODE3

We proceed with a non-linear case $\phi' = \lambda\phi(1-\phi)$ with stiff variations controlled by parameter $\lambda \in \mathbb{R}$. The solution is the sigmoid function $\phi(t) = \frac{1}{1+\exp(-\lambda t)}$ that presents a strong variation around $t = 0$ when λ is large. We solve the ODE by prescribing $\phi_0 = \phi(-1)$ and computing the solution over the interval $[-1, 1]$ using a Picard fixed point at each time step. The aim of the benchmark is to assess the robustness and accuracy of the solution after the sharp transition that takes place at $t = 0$. Several values for λ have been tested but we only report the two representative cases with $\lambda = 5$ (benchmark ODE3a) and $\lambda = 10$ (benchmark ODE3b). We plot in Fig. 9 the computed values for Z, D, and S and draw the exact solution and its derivatives.

Errors and convergence orders are reported in Tables 4 and 5 for the two situations, respectively. Notice that we compute the L_∞ norm over the whole time interval to measure the error at the transition. Expected orders of convergences are achieved and we observe the strong impact of the value of λ on the errors. Indeed, benchmark ODE3a produces lower errors of three magnitude orders comparing with benchmark ODE3b on the same meshes. Note also that now the errors of schemes [2ZD] and [1ZDS] are slightly different due to the non-linear nature of the benchmark.

3.4. Benchmark ODE4

We explore the system case and consider the first-order plane waves equation system

$$\begin{cases} \phi' = \alpha\psi, \\ \psi' = -\alpha\phi, \end{cases}$$

leading to the second-order linear equation $\phi'' + \alpha^2\phi = 0$, where $\alpha \in \mathbb{R}$. Assuming that $\phi(0) = 1$ and $\psi(0) = 0$, the exact solution reads $\phi(t) = \cos(\alpha t)$.

We consider a low frequency case $\alpha = 2.1\pi$ (benchmark ODE4a) and a high frequency case $\alpha = 10.1\pi$ (benchmark ODE4b) to check the ability of the schemes to catch the correct solution with low phase deviations. Tables 6 and 7 report the errors and convergence orders at the final time $T = 1$ for the five schemes. We just mention that no stability problems have been detected for the two conditionally stable schemes [2ZDS′] and [2ZDS″]. On the other hand, we perfectly recover the expected orders for the function and its derivatives except for scheme [2ZDS″] that provides a slightly better accuracy. Of course, the high frequency case provides pronounced errors for $N = 5, 10$ (particularly the second derivative). Indeed, if the time step Δt is larger than the characteristic time $1/\alpha$, we cannot "physically" catch the curved (we need at least 2 or 3 nodes in a complete revolution).

3.5. Comparison with other schemes

A comparison between the proposed schemes with traditional or recent methods for ordinary differential equations is proposed. Several criteria shall be assessed such as accuracy, dispersion, stability, and computational effort.

3.5.1. Description of the methods

Runge-Kutta methods are widely used in non-stationary problems. Other usual choices are multistep methods (Adams' family and Backward Differentiation Formula) that represent alternative techniques to reduce the computational cost compared with Diagonal Implicit RK (DIRK) when unconditional stability is an issue. Despite the fame of all

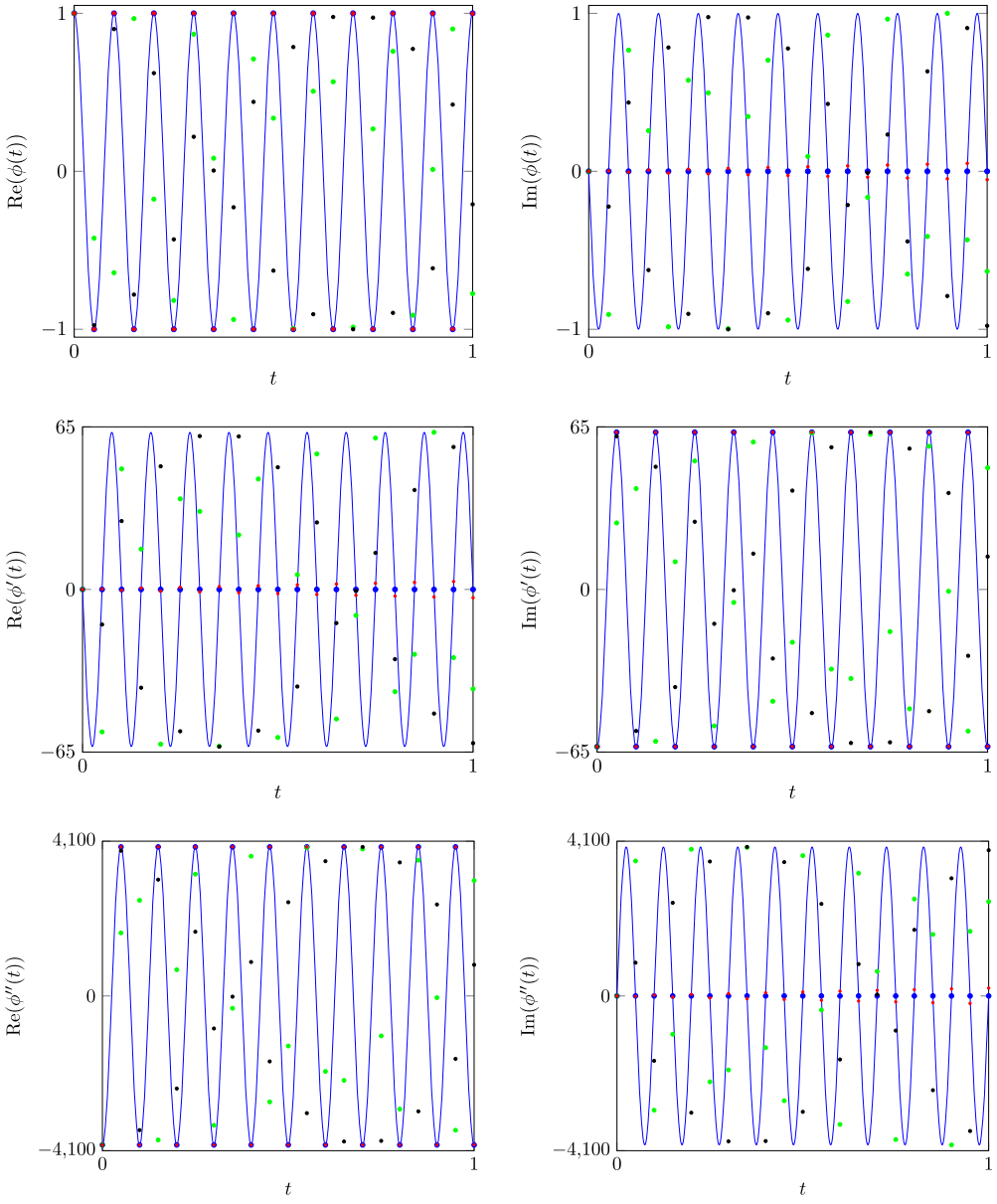

Fig. 7. Benchmark ODE2b: real (left) and imaginary (right) parts of ϕ (top), ϕ' (middle), and ϕ'' (bottom): exact solution $\phi(t)$ (——), exact solution at $t = \frac{i}{N}$ (•), [CN] numerical solution at $t = \frac{i}{N}$ (•), [2ZD] numerical solution at $t = \frac{i}{N}$ (•), and [2ZDS] numerical solution at $t = \frac{i}{N}$ (•), $N = 20$ and $i = 0, \ldots, N$.

these schemes, we propose to draw a comparison with the Donea, Roig, Huerta scheme [32] that presents some similarities with our schemes.

Based on the Padé representation of the exponential function, the authors present a list of unconditional, very high-order accurate schemes. We present the fourth-order and sixth-order versions corresponding to the [R22] and [R33] approximations, respectively:

- [R22] scheme, also proposed by Harten and Tal-Ezer in 1981 [33]:

$$\text{explicit stages} \begin{cases} \phi_{n+\frac{1}{6}} = \phi_n + \frac{\Delta t}{6} f(\phi_n, t_n) \\ \phi_{n+\frac{1}{2}} = \phi_n + \frac{\Delta t}{2} f(\phi_{n+\frac{1}{6}}, t_n + \frac{\Delta t}{6}) \end{cases}$$

$$\text{implicit stages} \begin{cases} \phi_{n+\frac{5}{6}} - \phi_{n+1} + \frac{\Delta t}{6} f(\phi_{n+1}, t_n + \Delta t) = 0 \\ \phi_{n+1} - \frac{\Delta t}{2} f(\phi_{n+\frac{5}{6}}, t_n + \frac{5\Delta t}{6}) = \phi_{n+\frac{1}{2}} \end{cases}$$

- [R33] scheme:

$$\text{explicit stages} \begin{cases} \phi_{n+\frac{1}{12}} = \phi_n + \frac{\Delta t}{12} f(\phi_n, t_n) \\ \phi_{n+\frac{1}{5}} = \phi_n + \frac{\Delta t}{5} f(\phi_{n+\frac{1}{12}}, t_n + \frac{\Delta t}{12}) \\ \phi_{n+\frac{1}{2}} = \phi_n + \frac{\Delta t}{2} f(\phi_{n+\frac{1}{5}}, t_n + \frac{\Delta t}{5}) \end{cases}$$

$$\text{implicit stages} \begin{cases} \phi_{n+\frac{11}{12}} - \phi_{n+1} + \frac{\Delta t}{12} f(\phi_{n+1}, t_n + \Delta t) = 0 \\ \phi_{n+\frac{4}{5}} - \phi_{n+1} + \frac{\Delta t}{5} f(\phi_{n+\frac{11}{12}}, t_n + \frac{11\Delta t}{12}) = 0 \\ \phi_{n+1} - \frac{\Delta t}{2} f(\phi_{n+\frac{4}{5}}, t_n + \frac{4\Delta t}{5}) = \phi_{n+\frac{1}{2}} \end{cases}$$

Note that the implicit part of [R22] involves two unknowns, as we do with the [1ZDS] scheme, while the implicit part of [R33] involves three unknowns when we need four unknowns in the [2ZDS] scheme.

General Linear Methods were designed by Butcher in [34] to be a unifying framework for Runge-Kutta methods and linear multi-step methods. We also have implemented two fourth-order schemes from

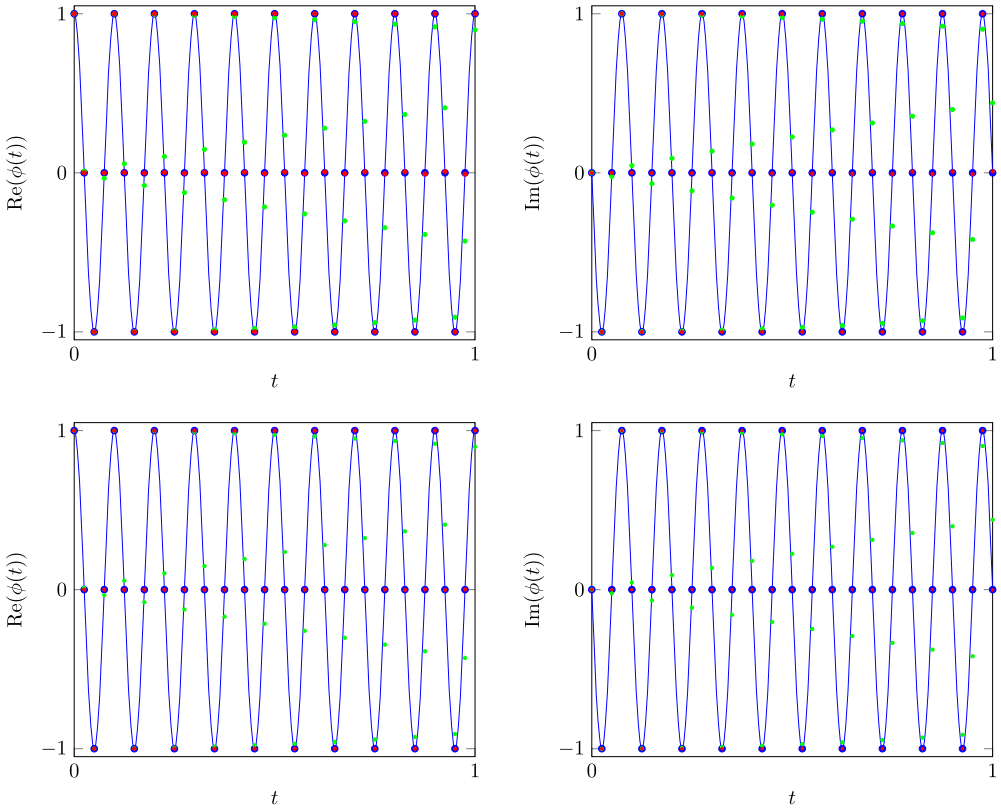

Fig. 8. Benchmark ODE2b: real (left) and imaginary (right) parts of ϕ with exact solution $\phi(t)$ (——) with (●) at the grid points, $N = 40$. Top panels: [R22] numerical solution (●) and [R33] numerical solution (●) at the grid points. Bottom panels: [1ZDS] numerical solution (●) and [2ZDS] numerical solution (●) at the grid points.

Table 4
Benchmark ODE3a.

time scheme	N	$\bar{k}$	Z		D		S	
			E_∞	O_∞	E_∞	O_∞	E_∞	O_∞
[2ZD]	5	18.00	7.69E−03	—	1.81E−02	—	3.32E−02	—
	10	12.10	4.80E−04	4.00	1.05E−03	4.11	5.99E−03	2.47
	20	9.60	3.01E−05	4.00	7.22E−05	3.86	3.65E−04	4.04
	30	8.67	5.93E−06	4.00	1.41E−05	4.03	7.17E−05	4.01
	40	8.00	1.87E−06	4.02	4.48E−06	3.99	2.26E−05	4.01
[1ZDS]	5	25.60	3.09E−03	—	7.09E−03	—	1.91E−02	—
	10	15.70	1.97E−04	3.97	4.55E−04	3.96	1.07E−03	4.15
	20	11.60	1.28E−05	3.95	2.80E−05	4.02	1.31E−04	3.03
	30	10.10	2.69E−06	3.84	5.50E−06	4.01	2.44E−05	4.15
	40	9.47	8.50E−07	4.01	1.74E−06	4.00	8.17E−06	3.80
[2ZDS]	5	21.40	1.47E−04	—	3.39E−04	—	6.58E−04	—
	10	13.90	8.19E−07	7.49	1.92E−06	7.46	6.64E−06	6.63
	20	10.85	1.75E−08	5.55	2.74E−08	6.13	1.79E−07	5.21
	30	9.63	1.42E−09	6.18	2.29E−09	6.12	1.51E−08	6.10
	40	8.97	2.38E−10	6.21	3.98E−10	6.08	2.44E−09	6.33
[2ZDS']	5	15.20	1.56E−03	—	7.73E−03	—	6.29E−01	—
	10	12.00	4.81E−05	5.02	1.11E−04	6.12	7.69E−02	3.03
	20	9.90	3.04E−06	3.99	7.02E−06	3.99	1.85E−02	2.05
	30	9.00	6.01E−07	4.00	1.45E−06	3.88	8.17E−03	2.02
	40	8.62	1.90E−07	4.00	4.67E−07	3.95	4.58E−03	2.01
[2ZDS"]	5	15.20	1.44E−03	—	3.34E−03	—	1.20E−02	—
	10	12.00	5.47E−05	4.72	1.26E−04	4.72	3.51E−04	5.09
	20	9.90	3.20E−06	4.10	7.12E−06	4.15	3.28E−05	3.42
	30	9.00	6.76E−07	3.83	1.39E−06	4.04	5.99E−06	4.19
	40	8.62	2.13E−07	4.01	4.36E−07	4.02	2.04E−06	3.75

Table 5
Benchmark ODE3b.

time scheme	N	$\bar{k}$	Z		D		S	
			E_∞	O_∞	E_∞	O_∞	E_∞	O_∞
[2ZD]	5	100.00	1.00E+00	—	1.05E+00	—	8.00E+00	—
	10	17.50	4.24E−02	4.56	1.40E−01	2.91	2.11E+00	1.92
	20	11.15	2.29E−03	4.21	8.69E−03	4.01	1.15E−01	4.20
	30	9.40	4.39E−04	4.07	1.79E−03	3.90	2.20E−02	4.07
	40	8.75	1.37E−04	4.04	5.54E−04	4.08	6.86E−03	4.04
[1ZDS]	5	39.00	3.10E−01	—	1.40E+00	—	7.21E+00	—
	10	26.70	3.29E−02	3.24	1.11E−01	3.65	1.64E+00	2.14
	20	15.15	1.83E−03	4.17	7.33E−03	3.92	9.13E−02	4.17
	30	12.27	3.51E−04	4.07	1.45E−03	4.00	1.75E−02	4.07
	40	10.88	1.12E−04	3.96	4.40E−04	4.13	5.50E−03	4.03
[2ZDS]	5	100.00	1.00E+00	—	1.05E+00	—	8.00E+00	—
	10	21.30	1.53E−04	12.67	8.73E−04	10.23	7.65E−03	10.03
	20	13.30	1.44E−06	6.74	6.64E−06	7.04	6.58E−05	6.86
	30	11.17	1.61E−07	5.39	5.38E−07	6.20	5.70E−06	6.03
	40	10.15	3.05E−08	5.79	1.04E−07	5.70	1.25E−06	5.28
[2ZDS']	5	42.40	1.24E−01	—	1.39E+00	—	6.19E+01	—
	10	15.50	3.26E−03	5.25	3.25E−02	5.42	5.19E+00	3.57
	20	11.25	6.56E−05	5.64	6.56E−04	5.63	4.00E−01	3.70
	30	9.93	1.33E−05	3.94	1.33E−04	3.94	1.80E−01	1.97
	40	9.25	4.22E−06	3.98	4.22E−05	3.98	1.02E−01	2.00
[2ZDS"]	5	39.40	2.98E−02	—	2.36E−01	—	1.31E+00	—
	10	15.40	6.51E−04	5.52	2.09E−03	6.82	3.25E−02	5.33
	20	11.30	2.17E−04	1.58	1.00E−03	1.06	1.09E−02	1.58
	30	9.93	5.85E−05	3.23	2.39E−04	3.54	2.78E−03	3.36
	40	9.25	2.09E−05	3.58	8.26E−05	3.69	9.86E−04	3.60

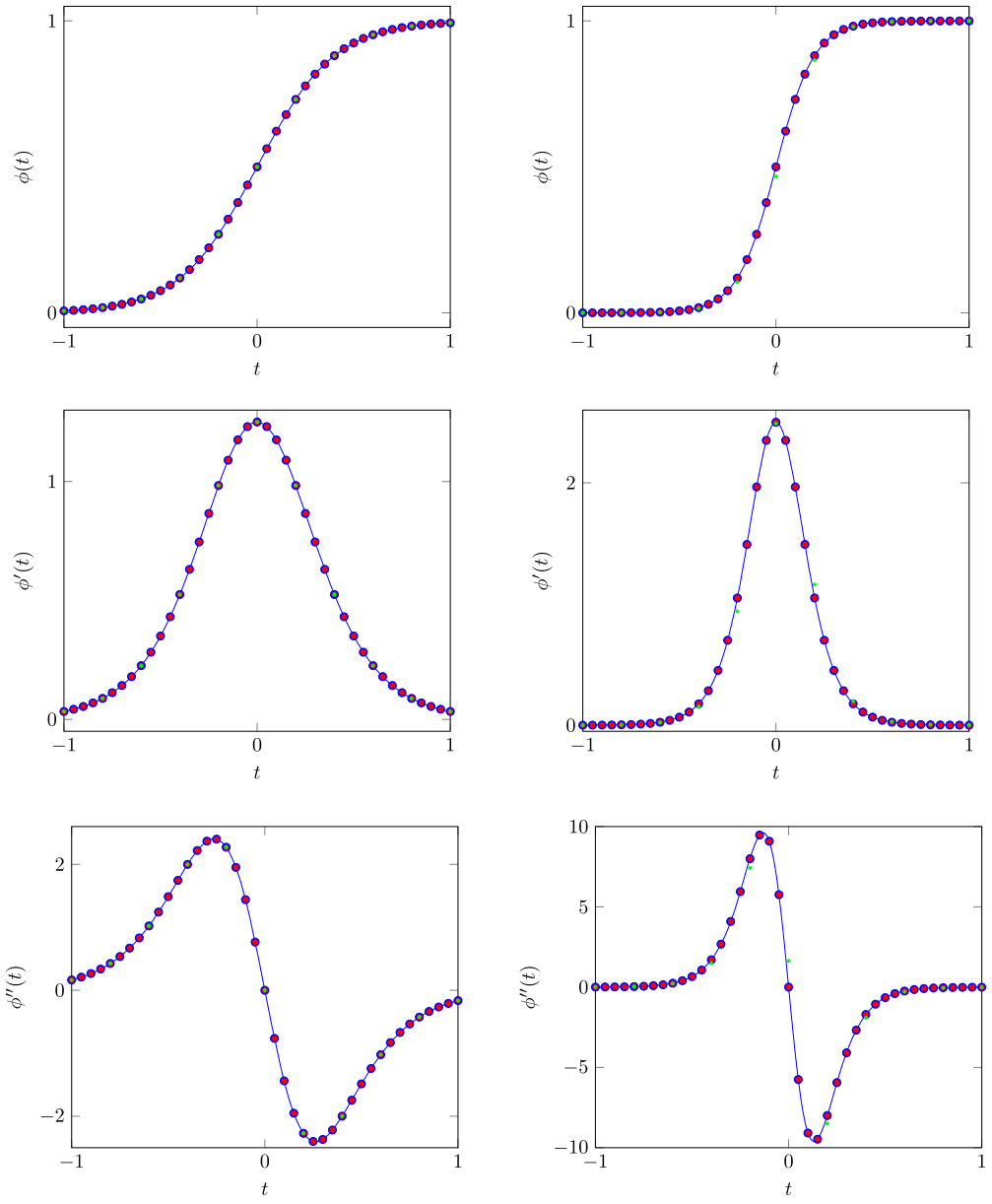

Fig. 9. Benchmark ODE3a — $\lambda = 5$ (left) and Benchmark ODE3b — $\lambda = 10$ (right) of ϕ (top), ϕ' (middle), and ϕ'' (bottom): exact solution (——), exact solution at $t = \frac{i}{N}$ (•), and `[1ZDS]` numerical solution at $t = \frac{i}{N}$ with $N = 10$ (•) and $N = 40$ (•), $i = 0, \dots, N$.

this recent family, denoted by `[GLM1]` and `[GLM2]`, which we compare with the `[1ZDS]` method.

- `[GLM1]` scheme
  The method is an Almost Runge-Kutta (ARK) technique introduced by Butcher in [35] and represents a particular case of the General Linear Method framework. We write using the author notations:

$$Y_1 = y_{n-1} + \frac{5}{8}\Delta t f(y_{n-1}) - \frac{1}{8}\Delta t f(y_{n-2}),$$

$$Y_2 = y_{n-1} - \frac{3}{2}\Delta t f(y_{n-1}) + \frac{1}{2}\Delta t f(y_{n-2}) + 2\Delta t f(Y_1),$$

$$y_n = y_{n-1} + \frac{1}{6}\Delta t f(y_{n-1}) + \frac{2}{3}\Delta t f(Y_1) + \frac{1}{6}\Delta t f(Y_2).$$

  The stability region of the method is the same of the classical fourth order Runge-Kutta method.
- `[GLM2]` scheme
  The second example is a fourth-order filtered implicit midpoint rule (MP-Pre-Post-4), recently presented in [36] and given by, using the author notations:

$$Y_1 = -\frac{1}{12}y_{n-4} + \frac{1}{2}y_{n-3} - \frac{5}{4}y_{n-2} + \frac{11}{6}y_{n-1},$$

$$Y_2 = Y_1 + \frac{1}{2}\Delta t f(Y_2),$$

$$Y_3 = 2Y_2 - Y_1,$$

$$y_n = -\frac{2}{25}y_{n-4} + \frac{2}{5}y_{n-3} - \frac{21}{25}y_{n-2} + \frac{26}{25}y_{n-1} + \frac{12}{25}Y_3.$$

  The method is $A(\alpha)$ stable with $\alpha = 70.64°$, (see Fig. 2 in [36]), which implies that the stability for imaginary numbers is conditioned since the domain of stability does not contain the entire line $i\mathbb{R}$.

3.5.2. Benchmarks

Convection-diffusion operators are characterised by imaginary and real eigenvalues by using the spectral decomposition, leading to a sys-

Table 6
Benchmark ODE4a.

time scheme	N	Z		D		S	
		E	O	E	O	E	O
[2ZD]	5	7.41E−03	—	1.57E−01	—	3.22E−01	—
	10	5.21E−04	3.83	1.06E−02	3.89	2.27E−02	3.83
	20	3.33E−05	3.97	6.76E−04	3.97	1.45E−03	3.97
	30	6.60E−06	3.99	1.34E−04	3.99	2.87E−04	3.99
	40	2.09E−06	4.00	4.25E−05	4.00	9.11E−05	4.00
[1ZDS]	5	7.41E−03	—	1.57E−01	—	3.22E−01	—
	10	5.21E−04	3.83	1.06E−02	3.89	2.27E−02	3.83
	20	3.33E−05	3.97	6.76E−04	3.97	1.45E−03	3.97
	30	6.60E−06	3.99	1.34E−04	3.99	2.87E−04	3.99
	40	2.09E−06	4.00	4.25E−05	4.00	9.11E−05	4.00
[2ZDS]	5	1.60E−05	—	3.26E−04	—	6.98E−04	—
	10	2.71E−07	5.89	5.50E−06	5.89	1.18E−05	5.89
	20	4.32E−09	5.97	8.76E−08	5.97	1.88E−07	5.97
	30	3.80E−10	5.99	7.72E−09	5.99	1.65E−08	5.99
	40	6.77E−11	6.00	1.38E−09	6.00	2.95E−09	6.00
[2ZDS′]	5	8.82E−04	—	1.11E−02	—	1.48E+00	—
	10	5.42E−05	4.02	5.12E−04	4.44	3.36E−01	2.14
	20	3.39E−06	4.00	2.92E−05	4.13	8.19E−02	2.04
	30	6.69E−07	4.00	5.68E−06	4.04	3.62E−02	2.01
	40	2.12E−07	4.00	1.79E−06	4.02	2.04E−02	2.01
[2ZDS″]	5	3.31E−03	—	4.33E−02	—	1.44E−01	—
	10	4.06E−05	6.35	2.90E−03	3.90	1.77E−03	6.35
	20	2.96E−06	3.78	1.79E−04	4.02	1.29E−04	3.78
	30	9.45E−07	2.81	3.49E−05	4.03	4.11E−05	2.81
	40	3.56E−07	3.40	1.09E−05	4.03	1.55E−05	3.40

Table 7
Benchmark ODE4b.

time scheme	N	Z		D		S	
		E	O	E	O	E	O
[2ZD]	5	1.95E+00	—	1.31E+01	—	1.96E+03	—
	10	1.39E+00	0.49	3.83E+01	—	1.40E+03	0.49
	20	4.61E−02	4.91	7.40E+00	2.37	4.64E+01	4.91
	30	1.46E−02	2.83	1.57E+00	3.83	1.47E+01	2.83
	40	5.06E−03	3.70	5.08E−01	3.91	5.09E+00	3.70
[1ZDS]	5	1.95E+00	—	1.31E+01	—	1.96E+03	—
	10	1.39E+00	0.49	3.83E+01	—	1.40E+03	0.49
	20	4.61E−02	4.91	7.40E+00	2.37	4.64E+01	4.91
	30	1.46E−02	2.83	1.57E+00	3.83	1.47E+01	2.83
	40	5.06E−03	3.70	5.08E−01	3.91	5.09E+00	3.70
[2ZDS]	5	4.43E−02	—	6.75E+00	—	4.46E+01	—
	10	8.99E−03	2.30	8.38E−01	3.01	9.05E+00	2.30
	20	2.23E−04	5.34	2.17E−02	5.27	2.24E−01	5.34
	30	2.13E−05	5.79	2.07E−03	5.79	2.14E−02	5.79
	40	3.89E−06	5.90	3.80E−04	5.90	3.92E−03	5.90
[2ZDS′]	5	8.39E+02	—	1.99E+03	—	6.90E+05	—
	10	1.59E−01	12.37	1.45E+01	7.10	2.97E+02	11.18
	20	7.55E−04	7.72	2.86E−01	5.66	6.35E+01	2.23
	30	2.58E−04	2.65	3.31E−02	5.32	2.31E+01	2.49
	40	9.49E−05	3.47	7.88E−03	4.99	1.21E+01	2.26
[2ZDS″]	5	4.07E+01	—	1.98E+03	—	4.10E+04	—
	10	2.06E+00	4.30	1.09E+01	7.50	2.08E+03	4.30
	20	4.28E−02	5.59	2.03E+00	2.43	4.31E+01	5.59
	30	4.51E−03	5.55	4.34E−01	3.81	4.54E+00	5.55
	40	7.55E−04	6.21	1.40E−01	3.94	7.60E−01	6.21

tem of linear differential equations with complex values. Consequently, we only consider the two following situations.

- Benchmark 1, tagged EDO1, tackles the problem $\phi' = -\lambda\phi$ with $\lambda > 0$, where we assess accuracy, stability, and computational effort for the diffusion operator.

Table 8
Benchmark ODE1: Accuracy comparison between [R22], [GLM1], [GLM2], and [1ZDS] methods for Z variable.

N	[R22]		[GLM1]		[GLM2]		[1ZDS]	
	E	O	E	O	E	O	E	O
10	5.11E−08	—	1.09E−06	—	6.86E−06	—	5.11E−08	—
20	3.19E−09	4.00	6.76E−08	4.01	5.00E−07	3.78	3.19E−09	4.00
40	2.00E−10	4.00	4.21E−09	4.01	3.31E−08	3.92	2.00E−10	4.00
80	1.25E−11	4.00	2.63E−10	4.00	2.12E−09	3.96	1.25E−11	4.00
160	7.77E−13	4.00	1.64E−11	4.00	1.34E−10	3.98	7.80E−13	4.00
320	3.95E−14	4.30	1.02E−12	4.00	8.40E−12	4.00	4.96E−14	3.98

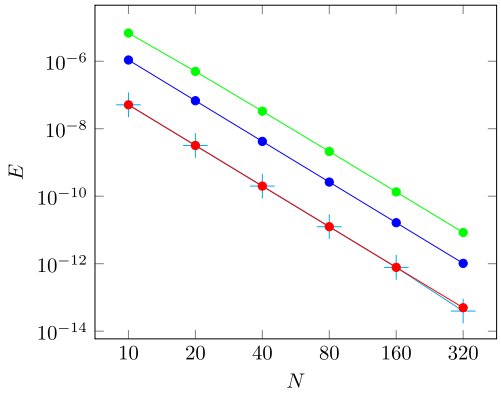

Fig. 10. Benchmark ODE1: Number of time steps versus error: [R22] ( ), [GLM1] ( ), [GLM2] ( ), and [1ZDS] ( ).

Table 9
Benchmark ODE1: Execution time comparison between [R22], [GLM1], [GLM2], and [1ZDS] methods.

N	[R22]	[GLM1]	[GLM2]	[1ZDS]
10	2.73E−04	1.86E−04	1.49E−04	3.73E−04
20	4.15E−04	3.44E−04	2.98E−04	5.75E−04
40	8.01E−04	6.91E−04	6.16E−04	1.11E−03
80	1.58E−03	1.36E−03	1.24E−03	2.19E−03
160	3.13E−03	2.77E−03	2.51E−03	4.30E−03
320	6.18E−03	5.47E−03	5.05E−03	8.69E−03

- Benchmark 2, tagged EDO2, tackles the problem $\phi' = -ik\pi\phi$ with $k > 0$, and aims to assess phase deviation, stability, and computational effort associated to the advection operator.

Fourth-order methods for the EDO1 benchmark
Simulations were carried out using the [R22], [GLM1], [GLM2], and [1ZDS] schemes with $\lambda = 1$. We report in Table 8 the error of accuracy together with the order, while we plot the convergence curves in Fig. 10. All the methods provide the expected fourth-order behaviour with the smallest accuracy error for [R22] and [1ZDS]. Execution times are given in Table 9 and Fig. 11 represents the computational effort with respect to the grid size. We observe some few advantages in favour of the [R22] method which we highlight with the curves of the running time versus accuracy error displayed in Fig. 12.

Fourth-order methods for the EDO2 benchmark
The phase deviation assesses the spectral resolution of the scheme and its capacity to resolve high frequencies with respect to Δt. Numerical simulations have been performed with $k = 10$ using successive grids (the coarsest being with $N = 40$, that is 8 points for a complete revolution). We present the phase deviation errors in Table 10 while we draw the phase deviation errors' curves in Fig. 13. Once again [R22] and [1ZDS] schemes provide the best results while the two General Linear methods we considered are less efficient. Computational effort in function of the grid size is evaluated in Table 11 and we plot the as-

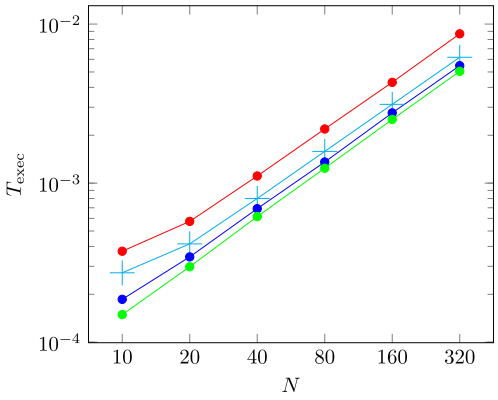

Fig. 11. Benchmark ODE1: Number of time steps versus execution time: [R22] ( ), [GLM1] ( ), [GLM2] ( ), and [1ZDS] ( ).

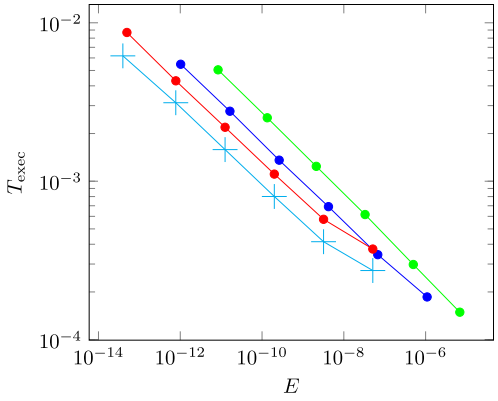

Fig. 12. Benchmark ODE1: Execution time versus error: [R22] ( ), [GLM1] ( ), [GLM2] ( ), and [1ZDS] ( ).

Table 10
Benchmark ODE2a: Comparison of phase errors between [R22], [GLM1], [GLM2], and [1ZDS] methods.

N	[R22]		[GLM1]		[GLM2]		[1ZDS]	
	E	O	E	O	E	O	E	O
40	1.60E−02	—	1.93E−01	—	1.93E−01	—	1.60E−02	—
80	1.03E−03	3.96	1.90E−02	3.35	1.31E−01	0.56	1.03E−03	3.96
160	6.47E−05	3.99	1.31E−03	3.86	1.04E−02	3.66	6.47E−05	3.99
320	4.05E−06	4.00	8.42E−05	3.96	6.87E−04	3.92	4.05E−06	4.00
640	2.53E−07	4.00	5.30E−06	3.99	4.37E−05	3.97	2.53E−07	4.00
1280	1.58E−08	4.00	3.32E−07	4.00	2.74E−06	3.99	1.58E−08	4.00

Table 11
Benchmark ODE2a: Comparison of execution time between [R22], [GLM1], [GLM2], and [1ZDS] methods.

N	[R22]	[GLM1]	[GLM2]	[1ZDS]
40	7.17E−04	6.51E−04	1.28E−03	9.55E−04
80	1.40E−03	1.32E−03	2.37E−03	1.75E−03
160	2.79E−03	2.57E−03	4.69E−03	3.43E−03
320	5.59E−03	5.22E−03	9.46E−03	6.85E−03
640	1.13E−02	1.04E−02	1.87E−02	1.37E−02
1280	2.25E−02	2.08E−02	3.71E−02	2.72E−02

sociated curves in Fig. 14. The running time is almost the same for all the methods, hence the comparison between phase deviation and running time in Fig. 15 gives the advantage to the [R22] scheme, and next, the [1ZDS] scheme.

Sixth-order methods

Concerning the sixth-order schemes, we only focus on the accuracy for the EDO1 problem reported in Table 12 and the phase deviation for the EDO2 equation given in Table 13. Due to the very high level of accuracy, it is reached to the limit of double precision even with a very low number of steps ($N = 2, \ldots, 8$, for the EDO1 test for instance). In both cases, [2ZDS] method shows a clear advantage regarded to the [R33] method with a gain of one magnitude.

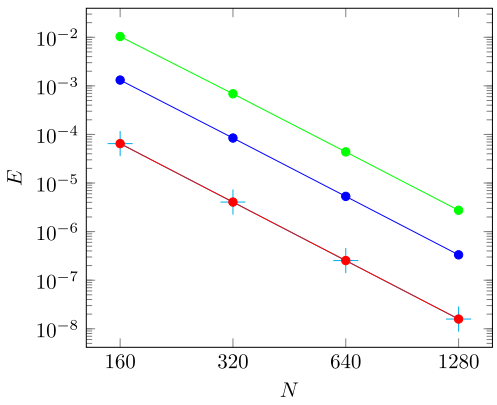

Fig. 13. Benchmark ODE2a: Number of time steps N versus phase errors: [R22] ( ), [GLM1] ( ), [GLM2] ( ), and [1ZDS] ( ).

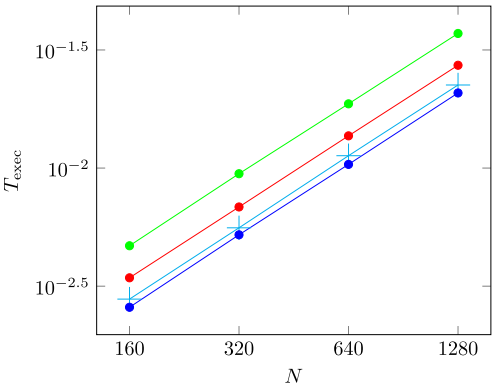

Fig. 14. Benchmark ODE2a: Number of time steps N versus execution time: [R22] ( ), [GLM1] ( ), [GLM2] ( ), and [1ZDS] ( ).

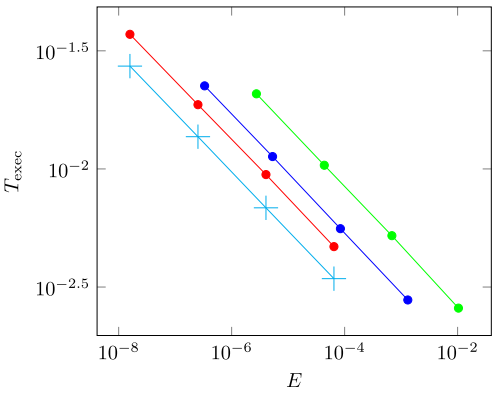

Fig. 15. Benchmark ODE2a: Execution time versus errors: [R22] ( ), [GLM1] ( ), [GLM2] ( ), and [1ZDS] ( ).

4. Benchmarking for partial differential equations

We extend the technology to PDEs, using a semi-discretization in space to provide a ODE system in time. Considering the one-dimensional case in space, we seek function $\phi = \phi(x,t)$ solution of

Table 12
Benchmark ODE1: Accuracy comparison between [R33] and [2ZDS] methods for Z variable.

N	[R33]		[2ZDS]	
	E	O	E	O
2	5.76E−08	—	9.64E−09	—
4	8.93E−10	6.01	1.49E−10	6.02
6	7.83E−11	6.00	1.31E−11	6.01
8	1.39E−11	6.00	2.32E−12	6.00

Table 13
Benchmark ODE2a: Phase error comparison between [R33] and [2ZDS] methods for Z variable.

N	[R33]		[2ZDS]	
	E	O	E	O
40	7.14E−05	—	1.18E−05	—
80	1.14E−06	5.97	1.89E−07	5.96
160	1.78E−08	5.99	2.97E−09	5.99
320	2.79E−10	6.00	4.65E−11	6.00
640	4.36E−12	6.00	7.25E−13	6.00
1280	6.98E−14	5.96	1.30E−14	5.81

$$\partial_t\phi + \partial_x F(\phi) = f, \quad \text{in } [0,L]\times(0,T],$$

where F is the physical flux, f is the source term, and $T>0$ is the final time. Since the focus of this work are time schemes, we eliminate boundary conditions issues considering that function ϕ is a L-periodic function in space. The equation is equipped with an initial condition $\phi(x,0)=\phi_0(x)$, $x\in[0,L]$. To achieve the discretization in space, we use the very simple centred finite difference method. To this end, let $I\in\mathbb{N}$ and $L=I\Delta x$. We denote $x_i=i\Delta x$, $i\in\mathbb{Z}$, a uniform discretization of the real axis. Due to L-periodicity, we have $\phi_{i+I}=\phi_i$, for all $i\in\mathbb{Z}$, hence the relevant data is only given by components ϕ_i, $i=1,\dots,I$.

For any time t, functions $Z_i(t)$, $D_i(t)$, and $S_i(t)$ are the approximations of $\phi(x_i,t)$, $\partial_t\phi(x_i,t)$, and $\partial_{tt}\phi(x_i,t)$, respectively, while vector $Z(t)=[Z_1(t),\dots,Z_I(t)]^{\mathrm{T}}$ gathers all the components (and similarly $D(t)$ and $S(t)$).

Regarding time discretization, let $N\in\mathbb{N}$, $\Delta t=T/N$, and $t_n=n\Delta t$. Therefore $Z_{i,n}$ states for an approximation of $\phi(x_i,t_n)$ at point x_i and time t_n, and we collect all the approximations in space with vector $Z_n=[Z_{1,n},\dots,Z_{I,n}]^{\mathrm{T}}$. Similarly, one has $D_n=[D_{1,n},\dots,D_{I,n}]^{\mathrm{T}}$ and $S_n=[S_{1,n},\dots,S_{I,n}]^{\mathrm{T}}$.

The point is to extend the high-order schemes for ODEs to the more general situation of PDEs. Basically the semi-discretization provides a semi-discrete linear or non-linear system

$$D(t)=\widehat{F}(Z(t),t),$$

where $\widehat{F}:\mathbb{R}^I\to\mathbb{R}^I$ characterizes the space operator discretization. Moreover, we prescribe the periodic boundary condition since we only focus on the time scheme and discard the additional difficulties related to the boundary conditions.

4.1. Linear convection-diffusion equation

We start with the simple linear convection-diffusion problem

$$\partial_t\phi - \kappa\partial_{xx}\phi + u\partial_x\phi = f, \quad \text{in } [0,L]\times(0,T], \tag{10}$$

where $u\in\mathbb{R}$ and $\kappa\geq 0$ are the velocity and diffusive coefficients, respectively. We tag this equation as PE1 (physical equation 1). A second physical equation (PE2) is obtained by deriving PE1 with respect to time and reads

$$\partial_{tt}\phi - \kappa\partial_{xx}(\partial_t\phi) + u\partial_x(\partial_t\phi) = \partial_t f. \tag{11}$$

At the semi-discrete level, equations (10)-(11) give

$$D(t) - \kappa A_{\mathrm{diff}} Z(t) + uA_{\mathrm{conv}} Z(t) - f(t) = 0,$$
$$S(t) - \kappa A_{\mathrm{diff}} D(t) + uA_{\mathrm{conv}} D(t) - f'(t) = 0,$$

where matrices A_{diff} and A_{conv} entries correspond to the finite discretization with a 9-point eighth-order centred scheme including the periodic condition for the diffusion and the convection operators. Source term vectors are given by

$$f(t)=\begin{bmatrix} f(x_1,t)\\ \dots\\ f(x_I,t)\end{bmatrix}, \qquad f'(t)=\begin{bmatrix} \partial_t f(x_1,t)\\ \dots\\ \partial_t f(x_I,t)\end{bmatrix}.$$

In addition to the physical equations PE1 and PE2, we consider the vector version of the Structural Equations by simply repeating the same linear combinations in time, for each node, since such relations are independent of i. By that way, we straightforward extend the schemes [2ZD], [1ZDS], and [2ZDS] to vectors Z_n, D_n, and S_n. As examples, we detail two representative situations with [2ZD] and [1ZDS].

- [2ZD] The two-stage ZD compact scheme is given by

$$\begin{aligned}
&D_{n+\frac12} + AZ_{n+\frac12} - f_{n+\frac12} = 0,\\
&D_{n+1} + AZ_{n+1} - f_{n+1} = 0,\\
&-6\frac{Z_{n+1}-Z_n}{\Delta t} + (D_n + 4D_{n+\frac12} + D_{n+1}) = 0,\\
&-4\frac{Z_n - 2Z_{n+\frac12} + Z_{n+1}}{\Delta t} + (D_{n+1} - D_n) = 0,
\end{aligned}$$

  with $A=-\kappa A_{\mathrm{diff}} + uA_{\mathrm{conv}}$. Vectors Z_0 and D_0 are the given initial functions. The problem recasts in the matrix formulation,

$$\begin{bmatrix} A & \mathrm{Id} & 0 & 0\\ 0 & 0 & A & \mathrm{Id}\\ 0 & 4\Delta t\mathrm{Id} & -6\mathrm{Id} & \Delta t\mathrm{Id}\\ 8\mathrm{Id} & 0 & -4\mathrm{Id} & \Delta t\mathrm{Id}\end{bmatrix}\begin{bmatrix} Z_{n+\frac12}\\ D_{n+\frac12}\\ Z_{n+1}\\ D_{n+1}\end{bmatrix} = \begin{bmatrix} 0 & 0\\ 0 & 0\\ -6\mathrm{Id} & -\Delta t\mathrm{Id}\\ 4\mathrm{Id} & \Delta t\mathrm{Id}\end{bmatrix}\begin{bmatrix} Z_n\\ D_n\end{bmatrix} + \begin{bmatrix} f_{n+\frac12}\\ f_{n+1}\\ 0\\ 0\end{bmatrix},$$

  where $4I\times 4I$ matrix gathers the convective and diffusive matrices together with the Structural Equations and Id representing the $I\times I$ identity matrix.
- [1ZDS] The one-stage ZDS compact scheme is given by

$$\begin{aligned}
&D_{n+1} + AZ_{n+1} - f_{n+1} = 0,\\
&S_{n+1} + AD_{n+1} - f'_{n+1} = 0,\\
&12\frac{Z_n - Z_{n+1}}{(\Delta t)^2} + 6\frac{D_n + D_{n+1}}{\Delta t} + (S_n - S_{n+1}) = 0,
\end{aligned}$$

  where Z_0, D_0, and S_0 are given initial functions. The problem recasts in the matrix formulation,

$$\begin{bmatrix} A & \mathrm{Id} & 0\\ 0 & A & \mathrm{Id}\\ 12\mathrm{Id} & -6\Delta t\mathrm{Id} & \Delta t^2\mathrm{Id}\end{bmatrix}\begin{bmatrix} Z_{n+1}\\ D_{n+1}\\ S_{n+1}\end{bmatrix} = \begin{bmatrix} 0 & 0 & 0\\ 0 & 0 & 0\\ 12\mathrm{Id} & 6\Delta t\mathrm{Id} & \Delta t^2\end{bmatrix}\begin{bmatrix} Z_n\\ D_n\\ S_n\end{bmatrix} + \begin{bmatrix} f_{n+1}\\ f'_{n+1}\\ 0\end{bmatrix},$$

  where the $3I\times 3I$ matrix gathers the convective and diffusive matrices together with the Structural Equations.

All the other schemes follow a similar matrix construction. To carry out the numerical simulations, the domain is the academic interval $[0,1]$ and we compute the solution until $T=1$. The space discretization corresponds to a eighth-order method with $I=40$. We manufactured a regular solution $\phi(x,t)=\sin(2\pi(x-2.1t))$ and compute the associated right hand-side term. Besides the ZDS schemes' family, we also consider in some benchmarks the classical [RK4] scheme to check the stability. The parts of the convergence tables regarding D and S for scheme [RK4] and S for scheme [2ZD] are computed *a posteriori* and printed again in blue (this notation is also followed on the other benchmarks).

Table 14
Benchmark PDE-CONVDIF1.

time scheme	N	Z		D		S	
		E_∞	O_∞	E_∞	O_∞	E_∞	O_∞
[2ZD]	20	1.06E−04	—	6.68E−04	—	4.20E−03	—
	25	4.37E−05	3.99	2.74E−04	3.99	1.72E−03	3.99
	30	2.11E−05	3.99	1.33E−04	3.99	8.33E−04	3.99
	35	1.14E−05	3.99	7.16E−05	3.99	4.50E−04	3.99
[1ZDS]	20	3.08E−04	—	1.94E−03	—	1.22E−02	—
	25	1.27E−04	3.99	7.95E−04	3.99	5.00E−03	3.99
	30	6.11E−05	3.99	3.84E−04	3.99	2.41E−03	3.99
	35	3.30E−05	3.99	2.08E−04	3.99	1.30E−03	3.99
[2ZDS]	20	1.60E−07	—	1.00E−06	—	6.30E−06	—
	25	4.18E−08	6.02	2.61E−07	6.03	1.63E−06	6.06
	30	1.38E−08	6.08	8.56E−08	6.12	5.27E−07	6.19
	35	5.29E−09	6.22	3.22E−08	6.33	1.99E−07	6.33

Table 15
Benchmark PDE-CONVDIF2.

time scheme	N	Z		D		S	
		E_∞	O_∞	E_∞	O_∞	E_∞	O_∞
[2ZD]	20	3.21E−04	—	1.28E−02	—	5.13E−01	—
	25	1.32E−04	3.97	5.29E−03	3.97	2.12E−01	3.97
	30	6.40E−05	3.99	2.56E−03	3.99	1.02E−01	3.99
	35	3.46E−05	3.99	1.38E−03	3.99	5.53E−02	3.99
[1ZDS]	20	8.55E−05	—	3.42E−03	—	1.37E−01	—
	25	3.52E−05	3.98	1.41E−03	3.98	5.62E−02	3.98
	30	1.70E−05	3.98	6.80E−04	3.98	2.72E−02	3.98
	35	9.20E−06	3.99	3.68E−04	3.99	1.47E−02	3.99
[2ZDS]	20	4.73E−08	—	1.89E−06	—	7.57E−05	—
	25	1.21E−08	6.11	4.85E−07	6.10	1.95E−05	6.09
	30	3.95E−09	6.14	1.60E−07	6.09	6.46E−06	6.05
	35	1.51E−09	6.24	6.19E−08	6.14	2.55E−06	6.02

Table 16
Benchmark PDE-CONVDIF3a.

time scheme	N	Z	D	S
		E_∞	E_∞	E_∞
[2ZD]	40	1.96E−05	7.73E−04	3.05E−02
	670	3.59E−10	9.79E−09	3.69E−07
	3700	1.11E−10	1.46E−09	2.20E−08
	3800	1.11E−10	1.46E−09	2.39E−08
[RK4]	40	—	—	—
	3700	1.08E+47	1.12E+51	1.17E+55
	3800	9.81E−11	1.59E−09	5.83E−08
[1ZDS]	40	5.22E−06	2.06E−04	8.14E−03
	670	1.29E−10	4.08E−09	1.05E−07
	3700	1.11E−10	1.47E−09	2.50E−08
	3800	1.11E−10	1.47E−09	2.69E−08
[2ZDS]	40	6.99E−10	2.57E−08	1.07E−06
	70	1.14E−10	5.31E−10	4.14E−08
	3700	1.11E−10	1.47E−09	2.69E−08
	3800	1.11E−10	1.46E−09	2.74E−08

The first benchmark PDE-CONVDIF1 concerns the pure convective case with $u = 1$ and $\kappa = 0$. Table 14 reports the errors and convergence rates. Observed fourth-order and sixth-order of accuracy are in line with the ODE case and prove that the time schemes produce the optimal orders.

The second benchmark PDE-CONVDIF2 deals with a combination of convection and diffusion terms with $u = 1$ and $\kappa = 1$. Table 15 evidences that the application of the diffusion do not produce stability problems and the optimal orders are preserved.

Table 17
Benchmark PDE-CONVDIF3b.

time scheme	N	Z		D		S	
		E_∞	O_∞	E_∞	O_∞	E_∞	O_∞
[2ZD]	20	3.14E−04	—	1.24E−02	—	4.89E−01	—
	25	1.29E−04	4.00	5.08E−03	4.00	2.01E−01	4.00
	30	6.20E−05	4.01	2.45E−03	4.01	9.66E−02	4.01
	35	3.34E−05	4.01	1.32E−03	4.01	5.21E−02	4.01
[1ZDS]	20	8.37E−05	—	3.31E−03	—	1.31E−01	—
	25	3.42E−05	4.01	1.35E−03	4.01	5.33E−02	4.01
	30	1.65E−05	4.00	6.52E−04	4.00	2.57E−02	4.00
	35	8.91E−06	4.00	3.52E−04	4.00	1.39E−02	4.00
[2ZDS]	20	4.62E−08	—	1.82E−06	—	7.20E−05	—
	25	1.18E−08	6.10	4.66E−07	6.11	1.84E−05	6.10
	30	3.91E−09	6.07	1.53E−07	6.10	6.10E−06	6.07
	35	1.55E−09	6.02	5.94E−08	6.15	2.40E−06	6.05

The third benchmark PDE-CONVDIF3 tackles the pure diffusive case, which is a more demanding situation for explicit schemes due to the Courant-Friedrichs-Lewy (CFL) condition. Indeed, we have carried out the same simulation for the conditionally stable explicit scheme [RK4] and we show in Table 16 that [RK4] is unstable until $N = 3700$ whereas stability is recovered for $N = 3800$. Such large number of time-steps negatively affect the computation costs. On the other hand, schemes [2ZD], [1ZDS], and [2ZDS] are always stable, and Table 17 provides the errors for $N = 20$, 25, 30, and 35. It is noticeable that scheme [RK4] with $N = 3800$ provides an error around 1E−10 for Z which we attribute to the error in space together with the conditioning of the global matrix. Notice that we reach to the same error for $N = 670$ with the fourth-order schemes [2ZD], [1ZDS] and $N = 70$ with the sixth-order scheme [2ZDS], *i.e.* with a very small number of time steps in regards to the number of steps required by the [RK4] stability. By dramatically reducing the number of steps, we strongly reduce the computational cost.

4.2. Linear Schrödinger equation

The linear Schrödinger equation represents a challenging issue for both the accuracy and the spectral resolution. Low dispersion is of major importance since the wave function is highly variable and one has to preserve all the frequencies for the sake of conservation (probability, density, momentum, energy). Curiously, most authors focus on the space discretization by developing low dispersion compact schemes [37], but the time discretization is a more critical issue since the frequency increases as the square of the wave length. Consequently, very low dispersion schemes in time is a fundamental issue.

As an example, we consider in this particular benchmark the space domain $[x_{\rm lf}, x_{\rm rg}]$ and the classical case of a null potential in the vacuum between two infinite potentials at points $x_{\rm lf}$ and $x_{\rm rg}$. The equation reads

$$\partial_t \phi - {\rm i}\partial_{xx}\phi = 0, \quad \text{in } [x_{\rm lf}, x_{\rm rg}] \times (0, T], \tag{12}$$

with boundary conditions $\phi(x_{\rm lf}, t) = \phi(x_{\rm rg}, t) = 0$. We tag (PE1) the first Physical equation (12) and produce the second Physical Equation (PE2) by derivation with respect to time

$$\partial_{tt}\phi - {\rm i}\partial_{xx}(\partial_t \phi) = 0. \tag{13}$$

At the semi-discrete level in space, equations (12)-(13) read

$$D(t) - {\rm i}AZ(t) = 0,$$

$$S(t) - {\rm i}AD(t) = 0,$$

where matrix A represents the discrete Hamiltonian operator using the eighth-order centred finite difference method.

To carry out the benchmark PDE-SCH, we consider the initial solution

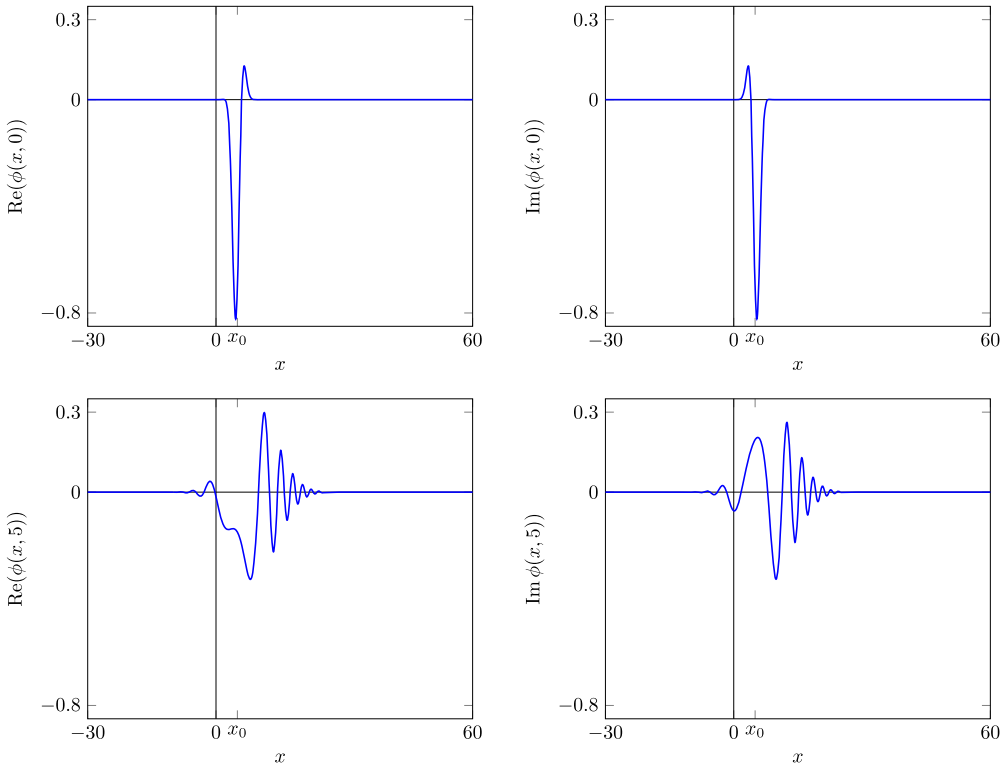

Fig. 16. Benchmark PDE-SCH: real (left) and imaginary (right) parts of $\phi(x,0)$ (top) and $\phi(x,5)$ (bottom).

$$\phi(x,0)=\frac{1}{\sqrt[4]{\sigma^2\pi}}\exp\left(-\left(\frac{x-x_0}{\sqrt{2}\sigma}\right)^2\right)\exp\left(\mathrm{i}k_\mathrm{c}\frac{x}{\hbar}\right),$$

being the exact solution given by

$$\phi(x,t)=\frac{1}{\sqrt[4]{\sigma^2\pi}}\frac{2\pi}{\sqrt{g(t)}}\exp\left(-\frac{(x-x_0-\frac{\hbar k_\mathrm{c}}{m}t)^2}{2g(t)\sigma^2}\right)\exp\left(-\mathrm{i}\frac{\hbar k_\mathrm{c}^2}{2m}t\right)\exp(\mathrm{i}k_\mathrm{c}x),$$

where $g(t)=1+\mathrm{i}\hbar\frac{t}{\sigma^2 m}$. Notice that we have the $\mathrm{i}k_\mathrm{c}^2$ term for the time whereas we just have a $\mathrm{i}k_\mathrm{c}$ term for the space, hence oscillations increase faster in time than space.

All the simulations have been carried out taking $\hbar=1$, $m=1$, $x_0=5$, $k_\mathrm{c}=\frac{\pi}{4}$, $\sigma=1$, with $x_\mathrm{lf}=-30$, $x_\mathrm{rg}=60$, and calculating until the final time $T=5$.

We plot in Fig. 16 the real and imaginary parts of $\phi(x,0)$ (top row) and $\phi(x,5)$ (bottom row) using a grid with $I=800$ nodes. We checked that the spatial step Δx is smaller than the minimal wave length and thus avoiding under-resolution frequencies. Table 18 reports the errors and convergence orders for the different schemes. As expected, the `[2ZD]` and `[1ZDS]` schemes enjoy a fourth-order of accuracy, while the errors for the `[2ZDS]` method are stalled for $N>50$ due to the lack of accuracy in space. We overcome the problem using a tenth-order in space discretization with $I=1000$, recovering the optimal sixth-order in time as can be observed in Table 19.

The above benchmark brings to the fore a nice additional property of the compact schemes: the asymptotic error $A(\Delta t)^\alpha$ has a smaller multiplicative constant A comparing with the constant B of the asymptotic error $B(\Delta t)^\beta$ of a conventional scheme (we mean without the derivatives). Using higher order derivatives as unknowns is the key for reducing the magnitude of the constant. Consequently, the conventional scheme order has to be higher than the compact scheme to achieve the same amount of errors. Such an issue holds when blending a compact scheme in time with a conventional scheme in space. We reinforce the argumentation with a comparison between the explicit `[RK4]` and the `[1ZDS]` schemes. Both are of fourth-order, but the stability condition requires that $N\geq 1500$ to provide a correct approximation in the `[RK4]` case. It is then noticeable that the `[1ZDS]` achieves the same error but with just $N=150$ as shown in Table 20. It highlights the advantages

Table 18
Benchmark PDE-SCH — version 1.

time scheme	N	Z		D		S	
		E_∞	O_∞	E_∞	O_∞	E_∞	O_∞
`[2ZD]`	30	3.61E−04	—	2.47E−03	—	1.97E−02	—
	40	1.16E−04	3.93	8.02E−04	3.92	6.40E−03	3.91
	50	4.83E−05	3.95	3.33E−04	3.94	2.67E−03	3.92
	60	2.35E−05	3.96	1.62E−04	3.95	1.30E−03	3.94
	70	1.27E−05	3.96	8.81E−05	3.95	7.08E−04	3.94
`[1ZDS]`	30	3.61E−04	—	2.47E−03	—	1.97E−02	—
	40	1.16E−04	3.93	8.01E−04	3.92	6.40E−03	3.91
	50	4.83E−05	3.95	3.33E−04	3.94	2.67E−03	3.92
	60	2.35E−05	3.96	1.62E−04	3.95	1.30E−03	3.94
	70	1.27E−05	3.96	8.81E−05	3.95	7.08E−04	3.95
`[2ZDS]`	30	5.89E−07	—	5.29E−06	—	5.27E−05	—
	40	8.53E−08	6.72	8.18E−07	6.49	8.61E−06	6.30
	50	2.53E−08	5.44	1.41E−07	7.88	1.22E−06	8.75
	60	3.68E−08	—	2.36E−07	—	1.74E−06	—
	70	4.13E−08	—	2.78E−07	—	2.16E−06	—

Table 19
Benchmark PDE-SCH — version 2.

time scheme	N	Z		D		S	
		E_∞	O_∞	E_∞	O_∞	E_∞	O_∞
`[2ZDS]`	30	6.24E−07	—	5.54E−06	—	5.48E−05	—
	40	1.17E−07	5.82	1.05E−06	5.77	1.06E−05	5.71
	50	3.14E−08	5.90	2.84E−07	5.87	2.88E−06	5.84
	60	1.05E−08	5.98	9.61E−08	5.95	9.79E−07	5.92
	70	4.13E−09	6.09	3.78E−08	6.06	3.87E−07	6.03

Table 20
Benchmark PDE-SCH — version 3.

time scheme	N	Z	D	S
		E_∞	E_∞	E_∞
[RK4]	1480	2.40E+13	2.02E+16	1.70E+19
	1500	5.78E−06	2.71E−05	1.58E−04
[1ZDS]	150	6.17E−06	3.02E−05	1.85E−04

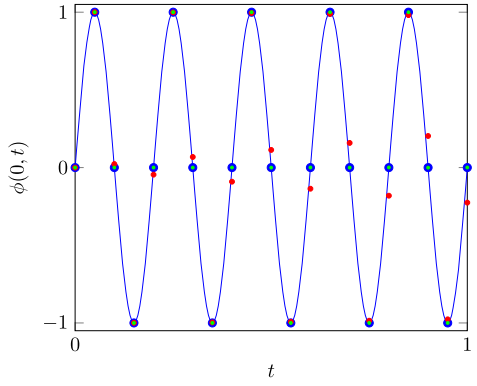

Fig. 17. Benchmark PDE-WAV for $x = 0$ and $t \in [0,1]$: exact solution $\phi(0,t)$ (——), exact solution at $t = \frac{i}{N}$ (•), [2ZD] numerical solution at $t = \frac{i}{N}$ (•), and [2ZDS] numerical solution at $t = \frac{i}{N}$ (•), $N = 20$ and $i = 0, \dots, N$.

of the ZDS class of schemes compared to the traditional Runge-Kutta of the same order.

4.3. Wave equation

Plane wave propagation is another important example where both diffusion and dispersion are critical issues. The linear wave propagation system reads

$$\partial_t \phi = c \partial_x \psi, \tag{14}$$

$$\partial_t \psi = -c \partial_x \phi, \tag{15}$$

where c is the propagation speed. We tag Physical Equation (14) as PE1$^\phi$ and Physical Equation (15) as PE1$^\psi$. The second physical equations (PE2$^\phi$ and PE2$^\psi$) come from the derivative with respect to time, and we get

$$\partial_{tt} \phi = c \partial_x (\partial_t \psi),$$

$$\partial_{tt} \psi = -c \partial_x (\partial_t \phi).$$

Denoting by A the eighth-order centred finite difference operator in space for the first-derivative, the semi-discretization of the four Physical Equations reads

$$D^\phi(t) - cAZ^\phi(t) = 0,$$

$$D^\psi(t) + cAZ^\psi(t) = 0,$$

$$S^\phi(t) - cAD^\phi(t) = 0,$$

$$S^\psi(t) + cAD^\psi(t) = 0.$$

For example, the [2ZD] method involves the Physical Equations PE1$^\phi$ and PE1$^\psi$ at time $t_{n+\frac{1}{2}}$ and t_{n+1} together with the two Structural Equations (6) and (7) **applied twice**: for Z^ϕ and D^ϕ on the one hand, for Z^ψ and D^ψ on the other hand. Similarly, to achieve the [1ZDS], we need the four Physical Equations at time t_{n+1} combined with equation (9) **applied twice**: Z^ϕ, D^ϕ, and S^ϕ for ϕ and Z^ψ, D^ψ, and S^ψ for ψ.

Table 21
Benchmark PDE-WAV.

time scheme	N	Z		D		S	
		E_∞	O_∞	E_∞	O_∞	E_∞	O_∞
[2ZD]	20	2.27E−01	—	7.13E+00	—	2.24E+02	—
	40	1.60E−02	3.83	5.02E−01	3.83	1.58E+01	3.83
	80	1.03E−03	3.96	3.23E−02	3.96	1.01E+00	3.96
	160	6.47E−05	3.99	2.03E−03	3.99	6.39E−02	3.99
[1ZDS]	20	2.27E−01	—	7.13E+00	—	2.24E+02	—
	40	1.60E−02	3.83	5.02E−01	3.83	1.58E+01	3.83
	80	1.03E−03	3.96	3.23E−02	3.96	1.01E+00	3.96
	160	6.47E−05	3.99	2.03E−03	3.99	6.39E−02	3.99
[2ZDS]	20	6.74E−04	—	2.12E−02	—	6.65E−01	—
	40	1.18E−05	5.84	3.69E−04	5.84	1.16E−02	5.84
	80	1.89E−07	5.96	5.93E−06	5.96	1.86E−04	5.96
	160	2.97E−09	5.99	9.33E−08	5.99	2.93E−06	5.99

To carry out the benchmark PDE-WAV, we consider the manufactured solution $\phi(x,t) = \sin(2\pi(x + ct))$ for a velocity $c = 5$. The domain is the simple interval $[0,1]$ with a grid of $I = 100$ nodes. Computations are carried out up to the final time $T = 1$. Table 21 provides the errors between the numerical approximations and the exact solution, together with the convergence order. To sum-up, the optimal orders are obtained for the different methods.

To assess the dispersion of the scheme, *i.e.* the phase deviation, we plot in Fig. 17 the solution and the approximations for the [2ZD] and [2ZDS] schemes along time at point $x = 0$ with $N = 20$. We clearly observe a delay with the fourth-order scheme while the sixth-order one perfectly match with the exact solution and demonstrate an excellent behaviour with respect to dispersion.

4.4. Bürgers' equation

We proceed with the scalar Bürgers' equation to evaluate the schemes' ability to handle non-linear problems. We aim at computing a numerical approximation of the Physical Equation (PE1)

$$\partial_t \phi - \phi \partial_x \phi = f, \quad \text{in } [0,L] \times (0,T], \tag{16}$$

where f represents a regular source term. Derivation in time provides the second Physical Equation (PE2)

$$\partial_{tt} \phi - \partial_t \phi \partial_x \phi - \phi \partial_x (\partial_t \phi) = \partial_t f. \tag{17}$$

At the semi-discrete level in space, equations (16)-(17) read

$$D(t) - Z(t)(AZ(t)) - f(t) = 0,$$

$$S(t) - D(t)(AZ(t)) - Z(t)(AD(t)) - f'(t) = 0,$$

where the product between vectors corresponds to the component-wise multiplication. Matrix A represents the eighth-order centred finite difference operator while $f(t)$ and $f'(t)$ are the vectors of the right hand side point-wise values for f and its time derivative.

We detail the [1ZDS] scheme as an example, the other methods proceed in a very similar way. The two Physical Equations are solved together with the Structural Equation leading to the non-linear system

$$D^{n+1} - Z^{n+1}(AZ^{n+1}) - f^{n+1} = 0,$$

$$S^{n+1} - D^{n+1}(AZ^{n+1}) - Z^{n+1}(AD^{n+1}) - f^{n+1\prime} = 0,$$

$$12\frac{Z^n - Z^{n+1}}{\Delta t^2} + 6\frac{D^n + D^{n+1}}{\Delta t} + (S^n - S^{n+1}) = 0.$$

We use a simple Picard fixed point method by computing a sequence $Z^{n,k}$, $D^{n,k}$, and $S^{n,k}$ until we achieve the convergence and provide the approximations at time t_{n+1}.

Benchmark PDE-BUR is achieved with the manufactured solution $\phi(x,t) = \sin(2\pi(x - 2.1t))$ on domain $[0,1]$, until the final time $T = 1$.

Table 22
Benchmark PDE-BUR.

time scheme	N	$\bar{k}$	Z		D		S	
			E_∞	O_∞	E_∞	O_∞	E_∞	O_∞
[2ZD]	30	11.00	4.39E−05	—	4.13E−04	—	1.29E−02	—
	40	10.00	1.38E−05	4.02	1.31E−04	3.99	4.11E−03	3.99
	50	10.00	5.64E−06	4.02	5.35E−05	4.00	1.68E−03	4.00
	60	9.00	2.71E−06	4.01	2.58E−05	4.00	8.11E−04	4.01
[1ZDS]	30	13.00	7.03E−05	—	4.60E−04	—	1.24E−02	—
	40	12.00	2.22E−05	4.00	1.46E−04	4.00	3.95E−03	3.99
	50	11.00	9.10E−06	4.00	5.97E−05	4.00	1.62E−03	4.00
	60	11.00	4.39E−06	4.00	2.88E−05	4.00	7.81E−04	3.99
[2ZDS]	30	11.97	1.63E−08	—	1.07E−07	—	2.89E−06	—
	40	11.00	2.89E−09	6.01	1.89E−08	6.01	5.13E−07	6.00
	50	10.98	7.56E−10	6.01	4.96E−09	6.01	1.35E−07	5.99
	60	10.00	2.53E−10	6.00	1.66E−09	6.00	4.51E−08	6.01

Space discretization uses a $I = 100$ node grid. We present in Table 22 errors and convergence orders. We also mention the average number of iterations k for the Picard fixed point to solve the non-linear system at each time step. One observes that $\bar{k}$ slightly decreases with N and seems scheme independent. Moreover, we find out the optimal order for the function and derivatives. Again the errors of schemes [2ZD] and [1ZDS] are slightly different due to the non-linear nature of the benchmark.

4.5. Euler system

With the last benchmark, we tackle the non-linear one-dimensional Euler system which represents a real and important problem for the CFD community. We seek regular solutions for the density ρ, velocity u, and pressure p of the Physical Equations PE1$^\rho$, PE1^u, and PE1^p

$$\partial_t \rho + u\partial_x \rho + \rho \partial_x u = f_\rho, \tag{18}$$

$$\partial_t u + u\partial_x u + \frac{1}{\rho}\partial_x p = f_u, \quad \text{in } [0, L]\times(0, T], \tag{19}$$

$$\partial_t p + u\partial_x p + \gamma p \partial_x u = f_p, \tag{20}$$

where f_ρ, f_u, and f_p represent source terms. A second set of Physical Equations is obtained by computing the derivative with respect to time and give

$$\partial_{tt}\rho + \partial_t u\partial_x \rho + u\partial_x(\partial_t \rho) + \partial_t \rho \partial_x u + \rho\partial_x(\partial_t u) = \partial_t f_\rho, \tag{21}$$

$$\partial_{tt} u + \partial_t u\partial_x u + u\partial_x(\partial_t u) - \frac{\partial_t \rho}{\rho^2}\partial_x p + \frac{1}{\rho}\partial_x(\partial_t p) = \partial_t f_u, \tag{22}$$

$$\partial_{tt} p + \partial_t u\partial_x p + u\partial_x(\partial_t p) + \gamma \partial_t p \partial_x u + \gamma p\partial_x(\partial_t u) = \partial_t f_p. \tag{23}$$

At the space discrete level, equations (18)-(20) read

$$D^\rho(t) + Z^u(t)(AZ^\rho(t)) + Z^\rho(t)(AZ^u(t)) - f_\rho(t) = 0,$$

$$D^u(t) + Z^u(t)(AZ^u(t)) + \frac{1}{Z^\rho(t)}(AZ^p(t)) - f_u(t) = 0,$$

$$D^p(t) + Z^u(t)(AZ^p(t)) + \gamma Z^p(t)(AZ^u(t)) - f_p(t) = 0,$$

where matrix A corresponds to the eighth-order centred finite differences in space. Of course, expressions of products and fractions are performed component-wise. Equations for the system (21)-(23) read

$$S^\rho(t) + D^u(t)(AZ^\rho(t)) + Z^u(t)(AD^\rho(t)) + D^\rho(t)(AZ^u(t)) + Z^\rho(t)(AD^u(t)) - f'_\rho(t) = 0,$$

$$S^u(t) + D^u(t)(AZ^u(t)) + Z^u(t)(AD^u(t)) + \frac{D^\rho(t)}{(Z^\rho(t))^2}(AZ^p(t)) + \frac{1}{Z^\rho(t)}AD^p(t) - f'_u(t) = 0,$$

$$S^p(t) + D^u(t)AZ^p(t) + Z^u(t)AD^p(t) + \gamma D^p(t)AZ^u(t) + \gamma Z^p(t)AD^u(t) - f'_p(t) = 0.$$

Table 23
Benchmark PDE-EUL1 — density.

time scheme	N	$\bar{k}$	Z		D		S	
			E_∞	O_∞	E_∞	O_∞	E_∞	O_∞
[2ZD]	20	14.00	2.37E−03	—	8.30E−02	—	5.93E+00	—
	30	12.00	2.60E−04	5.45	1.31E−02	4.55	8.81E−01	4.70
	40	11.00	9.41E−05	3.54	3.71E−03	4.38	2.71E−01	4.10
	50	10.84	4.23E−05	3.58	1.77E−03	3.32	1.08E−01	4.12
[1ZDS]	20	15.95	1.83E−03	—	5.05E−02	—	3.08E+00	—
	30	14.03	3.81E−04	3.87	1.11E−02	3.74	6.19E−01	3.96
	40	14.35	1.16E−04	4.14	3.82E−03	3.70	2.58E−01	3.05
	50	11.72	4.69E−05	4.06	1.79E−03	3.39	1.17E−01	3.53
[2ZDS]	20	12.45	9.23E−07	—	4.38E−05	—	3.46E−03	—
	30	11.00	8.44E−08	5.90	5.06E−06	5.32	4.42E−04	5.08
	40	11.00	1.45E−08	6.12	9.26E−07	5.90	8.02E−05	5.93
	50	10.00	3.79E−09	6.01	2.40E−07	6.05	2.14E−05	5.92

Table 24
Benchmark PDE-EUL1 — velocity.

time scheme	N	$\bar{k}$	Z		D		S	
			E_∞	O_∞	E_∞	O_∞	E_∞	O_∞
[2ZD]	20	14.00	9.48E−04	—	1.76E−02	—	1.29E+00	—
	30	12.00	1.66E−04	4.30	3.76E−03	3.81	2.47E−01	4.08
	40	11.00	5.34E−05	3.94	9.58E−04	4.75	7.59E−02	4.10
	50	10.84	2.18E−05	4.01	4.46E−04	3.43	2.81E−02	4.45
[1ZDS]	20	15.95	9.02E−04	—	1.71E−02	—	8.76E−01	—
	30	14.03	1.97E−04	3.75	3.84E−03	3.68	1.99E−01	3.65
	40	14.35	6.28E−05	3.98	9.19E−04	4.97	6.66E−02	3.81
	50	11.72	2.58E−05	3.99	4.29E−04	3.42	3.32E−02	3.13
[2ZDS]	20	12.45	5.51E−07	—	9.90E−06	—	7.37E−04	—
	30	11.00	5.06E−08	5.89	9.46E−07	5.79	9.77E−05	4.99
	40	11.00	8.91E−09	6.04	1.73E−07	5.90	1.74E−05	6.01
	50	10.00	2.34E−09	5.99	4.48E−08	6.06	4.64E−06	5.91

Table 25
Benchmark PDE-EUL1 — pressure.

time scheme	N	$\bar{k}$	Z		D		S	
			E_∞	O_∞	E_∞	O_∞	E_∞	O_∞
[2ZD]	20	14.00	1.32E−03	—	5.27E−02	—	4.19E+00	—
	30	12.00	2.32E−04	4.30	1.11E−02	3.85	7.88E−01	4.12
	40	11.00	8.11E−05	3.65	2.82E−03	4.75	2.48E−01	4.01
	50	10.84	3.18E−05	4.19	1.32E−03	3.39	9.23E−02	4.44
[1ZDS]	20	15.95	1.21E−03	—	5.09E−02	—	2.87E+00	—
	30	14.03	2.40E−04	3.99	1.13E−02	3.72	6.45E−01	3.68
	40	14.35	6.83E−05	4.38	2.62E−03	5.06	2.17E−01	3.79
	50	11.72	2.89E−05	3.86	1.23E−03	3.39	1.08E−01	3.14
[2ZDS]	20	12.45	6.06E−07	—	2.85E−05	—	2.36E−03	—
	30	11.00	5.42E−08	5.95	2.90E−06	5.64	3.14E−04	4.97
	40	11.00	9.68E−09	5.99	5.32E−07	5.89	5.74E−05	5.91
	50	10.00	2.53E−09	6.00	1.38E−07	6.06	1.54E−05	5.91

The introduction of the scheme in time is achieved in a very similar way to the Bürgers' case. We do not repeat for the sake of simplicity. The Picard fixed point is implemented and enables to compute all the approximations at time t_{n+1}, being given the approximation at time t_n.

The Benchmark PDE-EUL1 is carried out with the manufactured regular functions

$$\rho(x,t) = \sin(2\pi(x - 2.1t)) + 3,\ u(x,t) = \sin(2\pi(x - 2.2t)),$$

$$p(x,t) = \sin(2\pi(x - 2.3t)) + 2,$$

over the domain $[0, 1]$ until the final time $T = 1$. Discretization in space is given with a grid of $I = 100$ nodes. Tables 23, 24, and 25 report the

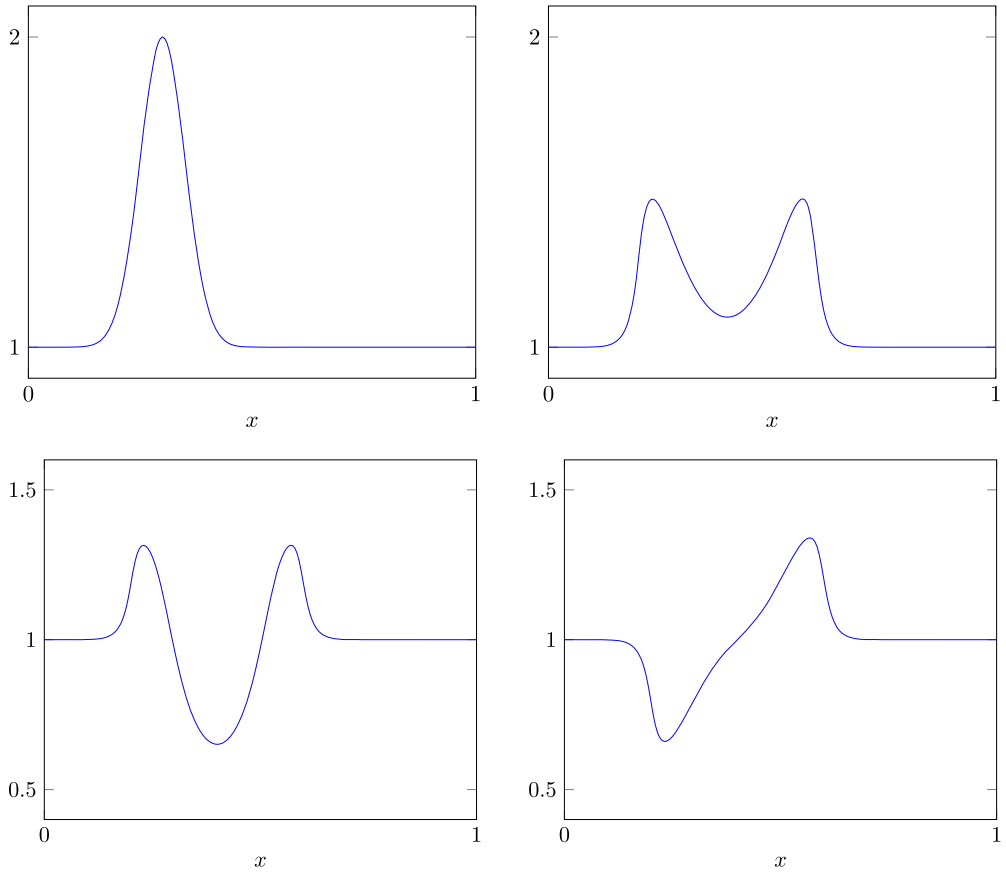

Fig. 18. Benchmark PDE-EUL2: top, left: initial pressure; top, right: numerical pressure at final time; bottom, left: numerical density at final time; bottom, right: numerical velocity at final time.

errors and the convergence orders for density, velocity, and pressure, respectively, considering the different time schemes. We also give the average number of Picard iterations $\bar{k}$ for solving the non-linear problem at each time step. We check that optimal orders in time are achieved with a small number of iterations to perform the fixed point procedure.

A second benchmark PDE-EUL2 consists to trace the evolution of an initial exponential bump of the pressure that splits into two smooth waves moving to the left and to the right, respectively. Moreover, we prescribe a positive initial fluid velocity such that the left wave is almost stationary. The initial condition then reads

$$\rho(x) = 1, \quad u(x) = 1, \quad p(x) = 1 + \exp\left(-\frac{(x - x_0)^2}{2\sigma^2}\right)$$

with $x_0 = 0.3$ the centre of the Gaussian bump and $\sigma = 0.05$ the standard deviation over the domain $[0, 1]$ until the final time $T = 0.1$ with $\gamma = 1.4$. Discretization in space is given with a grid of $I = 200$ and $N = 20$ time steps. Simulation is carried out with the eight-order finite difference scheme in space to guarantee a very small error in comparison with the fourth order `[2ZD]` scheme in time.

We report in Fig. 18 the initial pressure (top left panel) and the computed pressure at the final time (top right panel). Density and velocity at the final time are displayed at the bottom left and right panels, respectively. The solution has no analytical expression and remains smooth until $T = 0.1$. Note that discontinuities arise for larger time due to the compression of the waves.

5. Conclusion

Time discretization is usually a background topic and does not deserve enough attention. Topics such as wave propagation, Schrödinger equation, and electromagnetism involve high variation in time, which require high accuracy, low dispersion, and A-stable schemes. The present study introduces the compact scheme paradigm, almost used in space discretization, to design a new class of discretization schemes in time. We prove that we both achieve very high accuracy and low dispersion, while most of the methods enjoy the A-stability property. Benchmarks, combining the traditional finite difference method in space together with our proposed schemes, give evidences of the advantage of the structural and physical equations' combination. The concept will be extended to higher derivatives and time dependent boundary conditions will also be considered.

Data availability

No data was used for the research described in the article.

Acknowledgements

S. Clain and G.J. Machado acknowledge the financial support by Portuguese Funds through Foundation for Science and Technology (FCT) in the framework of the Strategic Funding UIDB/04650/2020.

M.T. Malheiro acknowledges the financial support by Portuguese Funds through Foundation for Science and Technology (FCT) in the framework of the Projects UIDB/00013/2020 and UIDP/00013/2020 of CMAT-UM.

S. Clain, G.J. Machado, and M.T. Malheiro acknowledge the financial support by FEDER – Fundo Europeu de Desenvolvimento Regional, through COMPETE 2020 – Programa Operacional Fatores de Competitividade, POCI-01-0145-FEDER-028118 and PTDC/MAT-APL/28118/2017.

References

[1] C.K. Tam, J.C. Webb, Dispersion relation preserving finite difference schemes for computational acoustics, J. Comput. Phys. 107 (2) (1993) 262–281, https://doi.org/10.1006/jcph.1993.1142.

[2] J.C. Butcher, Numerical Methods for Ordinary Differential Equations, 2nd edition, John Wiley & Sons Ltd, 2008.

[3] E. Hairer, G. Wanner, Solving Ordinary Differential Equations II: Stiff and Differential-Algebraic Problem, Springer Series in Computational Mathematics, Springer, Berlin, Heidelberg, 1996.

[4] G. Dahlquist, A special stability problem for linear multistep methods, BIT Numer. Math. 3 (1) (1963) 27–43, https://doi.org/10.1007/BF01963532.

[5] W. Boscheri, G. Dimarco, High order finite volume schemes with imex time stepping for the Boltzmann model on unstructured meshes, Comput. Methods Appl. Mech. Eng. 387 (2021) 114180, https://doi.org/10.1016/j.cma.2021.114180.

[6] W.B. Fritz, The iterative Simpson method of numerical integration, Technical Note no. 736, Aberdeen Proving Ground, 1952.

[7] E. Grabbe, S. Ramo, D. Woolridge, Handbook of Automation, Computation and Control, vol. 1: Control Fundamentals, Wiley Editor, New-York, 1958.

[8] J.D. Lambert, A.R. Mitchell, On the solution of $y' = f(x, y)$ by a class of high accuracy difference formulae of low order, Z. Angew. Math. Phys. 13 (1962) 223–232, https://doi.org/10.1007/BF01601084.

[9] J.D. Lambert, A.R. Mitchell, The use of higher derivatives in quadrature formulae, Comput. J. 5 (4) (1963) 322–327, https://doi.org/10.1093/comjnl/5.4.322.

[10] J.D. Lambert, Computational Methods in Ordinary Differential Equations, Academic Press, John Wiley & Sons, Cambridge, 1973.

[11] O. Axelsson, A class of a-stable methods, BIT Numer. Math. 9 (3) (1969) 185–199, https://doi.org/10.1007/BF01946812.

[12] L.F. Shampine, H.A. Watts, Block implicit one-step methods, Math. Comput. 23 (108) (1969) 731–740, http://www.jstor.org/stable/2004959.

[13] H.A. Watts, L.F. Shampine, A stable block implicit one-step methods, BIT Numer. Math. 12 (2) (1972) 252–266, https://doi.org/10.1007/BF01932819.

[14] E. Hairer, G. Wanner, Multistep-multistage-multiderivative methods for ordinary differential equations, Computing 11 (1973) 287–303, https://doi.org/10.1007/BF02252917.

[15] R.K. Sahi, S.N. Jator, N.A. Khan, A Simpson's type second derivative method for stiff systems, Int. J. Pure Appl. Math. 81 (4) (2012) 619–633, http://www.ijpam.eu.

[16] M.Y. Turki, F. Ismail, N. Senu, Z.B. Ibrahim, Two and three point implicit second derivative block methods for solving first order ordinary differential equations, ASM Sci. J. 12 (1) (2019) 10–23, http://psasir.upm.edu.my/id/eprint/82450.

[17] S. Fatunla, Block methods for second order odes, Int. J. Comput. Math. 41 (1–2) (1991) 55–63, https://doi.org/10.1080/00207169108804026.

[18] B.T. Olabode, An accurate scheme by block method for third order ordinary differential equations, Pac. J. Sci. Technol. 10 (1) (2009) 136–142.

[19] Y. Adam, A Hermitian finite difference method for the solution of parabolic equations, Comput. Math. Appl. 1 (3) (1975) 393–406, https://doi.org/10.1016/0898-1221(75)90041-3, https://www.sciencedirect.com/science/article/pii/0898122175900413.

[20] M.F. Pettigrew, On Compact Finite Difference Schemes with Applications to Moving Boundary Problems, Ph.D. thesis, Western University, 1989, https://ir.lib.uwo.ca/digitizedtheses/1847.

[21] S.K. Lele, Compact finite difference schemes with spectral-like resolution, J. Comput. Phys. 103 (1) (1992) 16–42, https://doi.org/10.1016/0021-9991(92)90324-R.

[22] P.C. Chu, C. Fan, A three-point combined compact difference scheme, J. Comput. Phys. 140 (1998) 370–399, https://doi.org/10.1006/JCPH.1998.5899.

[23] D.S. Watanabe, Block implicit one-step methods, Math. Comput. 32 (142) (1978) 405–414, http://www.jstor.org/stable/2006152.

[24] Q. Feng, B. Han, P. Minev, Sixth order compact finite difference schemes for Poisson interface problems with singular sources, Comput. Math. Appl. 99 (C) (2021) 2–25, https://doi.org/10.1016/j.camwa.2021.07.020.

[25] J. Li, Y. Chen, G. Liu, High-order compact adi methods for parabolic equations, Comput. Math. Appl. 52 (8) (2006) 1343–1356, https://doi.org/10.1016/j.camwa.2006.11.010.

[26] L. Qiao, D. Xu, W. Qiu, The formally second-order bdf adi difference/compact difference scheme for the nonlocal evolution problem in three-dimensional space, Appl. Numer. Math. 172 (C) (2022) 359–381, https://doi.org/10.1016/j.apnum.2021.10.021.

[27] D. Xu, W. Qiu, J. Guo, A compact finite difference scheme for the fourth-order time-fractional integro-differential equation with a weakly singular kernel, Numer. Methods Partial Differ. Equ. 36 (2) (2020) 439–458, https://doi.org/10.1002/num.22436.

[28] L. Qiao, W. Qiu, D. Xu, Error analysis of fast l1 adi finite difference/compact difference schemes for the fractional telegraph equation in three dimensions, Math. Comput. Simul. 205 (2023) 205–231, https://doi.org/10.1016/j.matcom.2022.10.001, https://ideas.repec.org/s/eee/matcom.html.

[29] R.P.K. Chan, A.Y.Y. Tsai, On explicit two-derivative Runge-Kutta methods, Numer. Algorithms 53 (2–3) (2010) 171–194, https://doi.org/10.1007/s11075-009-9349-1, https://researchspace.auckland.ac.nz/docs/uoa-docs/rights.htm.

[30] A.Y.J. Tsai, R.P.K. Chan, S. Wang, Two-derivative Runge–Kutta methods for pdes using a novel discretization approach, Numer. Algorithms 65 (2014) 687–703, https://doi.org/10.1007/s11075-014-9823-2.

[31] J. Li, Two-stage fourth order: temporal-spatial coupling in computational fluid dynamics (cfd), Adv. Aerodyn. 1 (3) (02 2019), https://doi.org/10.1186/s42774-019-0004-9.

[32] J. Donea, B. Roig, A. Huerta, High-order accurate time-stepping schemes for convection-diffusion problems, Comput. Methods Appl. Mech. Eng. 182 (3) (2000) 249–275, https://doi.org/10.1016/S0045-7825(99)00193-0.

[33] A. Harten, H. Tal-Ezer, On fourth-order accurate implicit finite difference schemes for hyperbolic conservation laws: I. Non-stiff strongly dynamic problems, Math. Comput. 36 (1981) 335–373, https://ui.adsabs.harvard.edu/abs/1981MaCom..36..353H.

[34] J.C. Butcher, General linear methods, Comput. Math. Appl. 31 (4/5) (1996) 105–112.

[35] J.C. Butcher, An introduction to "almost Runge-Kutta" methods, Appl. Numer. Math. 24 (2) (1997) 331–342, https://doi.org/10.1016/S0168-9274(97)00030-5.

[36] V. DeCaria, S. Gottlieb, Z.J. Grant, W.J. Layton, A general linear method approach to the design and optimization of efficient, accurate, and easily implemented time-stepping methods in cfd, J. Comput. Phys. 455 (2022) 110927, https://doi.org/10.1016/j.jcp.2021.110927.

[37] S.-S. Xie, G.-X. Li, S. Yi, Compact finite difference schemes with high accuracy for one-dimensional nonlinear Schrödinger equation, Comput. Methods Appl. Mech. Eng. 198 (2009) 1052–1060, https://doi.org/10.1016/J.CMA.2008.11.011.